Advanced Signal Processing Techniques For Full-Duplex Systems

Elyes Balti (ebalti@utexas.edu)
Wireless Networking and Communications Group (WNCG)
6G@UT Research Center
The University of Texas at Austin

Ph.D. Committee
Prof. Brian L. Evans (Supervisor)
Prof. Haris Vikalo
Prof. Ahmed Tewfik
Prof. Lili Qiu
Prof. Murat Torlak

November 18, 2024

Outline

Outline

Evolution of Cellular Communications

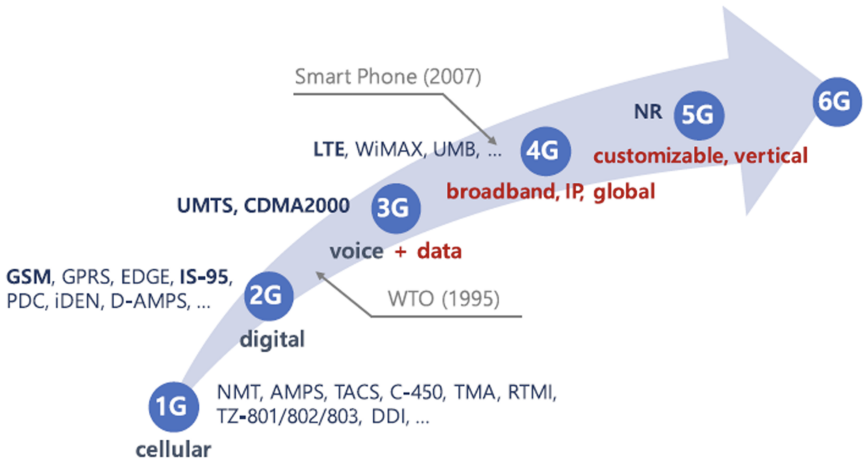

(a) Cellular network generations

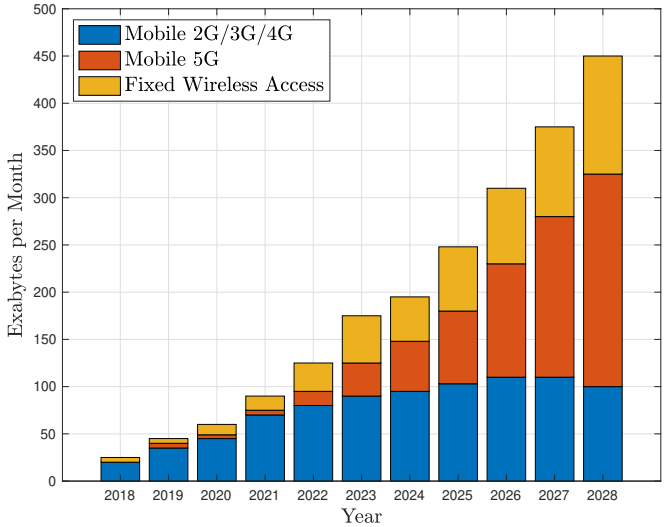

(b) Global mobile traffic forecast

Each generation means

- 10x increase in data rate
- More complex infrastructure
- More complex use cases

Samsung Research. *6G The Next Hyper-Connected Experience for All*.

A. Harutyunyan and P. Sen. In-Band Full-Duplex Solutions in the Paradigm of Integrated Sensing and Communication. In: *2023 IEEE Int. Conf. Acoustics, Speech, and Signal Processing Workshops*. 2023.

6G Services

(a) Truly Immersive XR

(b) High-fidelity Mobile Hologram

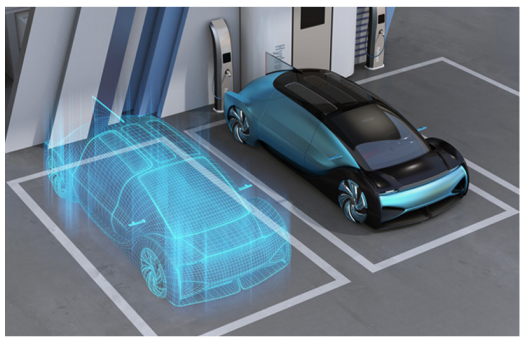

(c) Digital Twin

- **Truly Immersive XR**: Very high data rates and low latency to realize Virtual Reality, Augmented Reality, and Mixed Reality
- **High-fidelity Mobile Hologram**: Next-generation media technology presenting gestures and facial expressions by means of a holographic display
- **Digital Twin**: Replicates physical entities and interact with them in a virtual world without temporal or spatial constraints

---

Samsung Research. *6G The Next Hyper-Connected Experience for All*.

Examples of 6G Requirements/Challenges

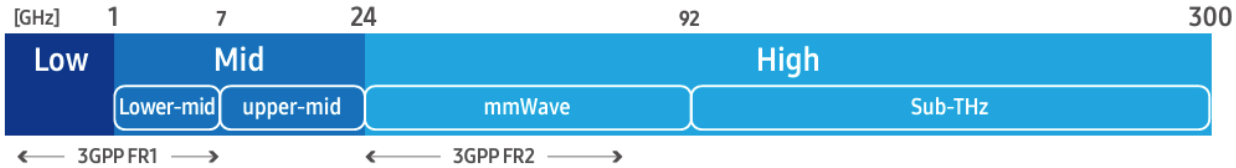

6G spectrum grouping

- Requirements:
  1. Peak data rate: 1 Tbps (5G x 50)
  2. Average data rate: 1 Gbps (5G x 10)
  3. Latency: 100 μsec (5G x $\frac{1}{10}$)
- Challenges:
  1. Severe path-loss (280 GHz has $\approx$ 20 dB higher than 28 GHz)
  2. Massive numbers of antennas to overcome severe path-loss
  3. More power consumption (e.g., ADC)

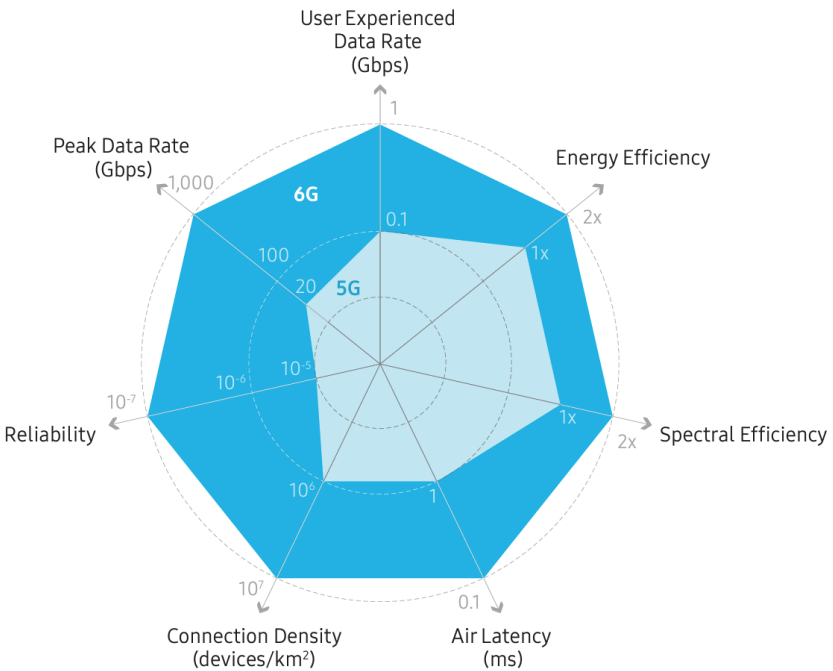

5G vs. 6G key performance requirements

Samsung Research. *6G The Next Hyper-Connected Experience for All*.

Duplex Technology

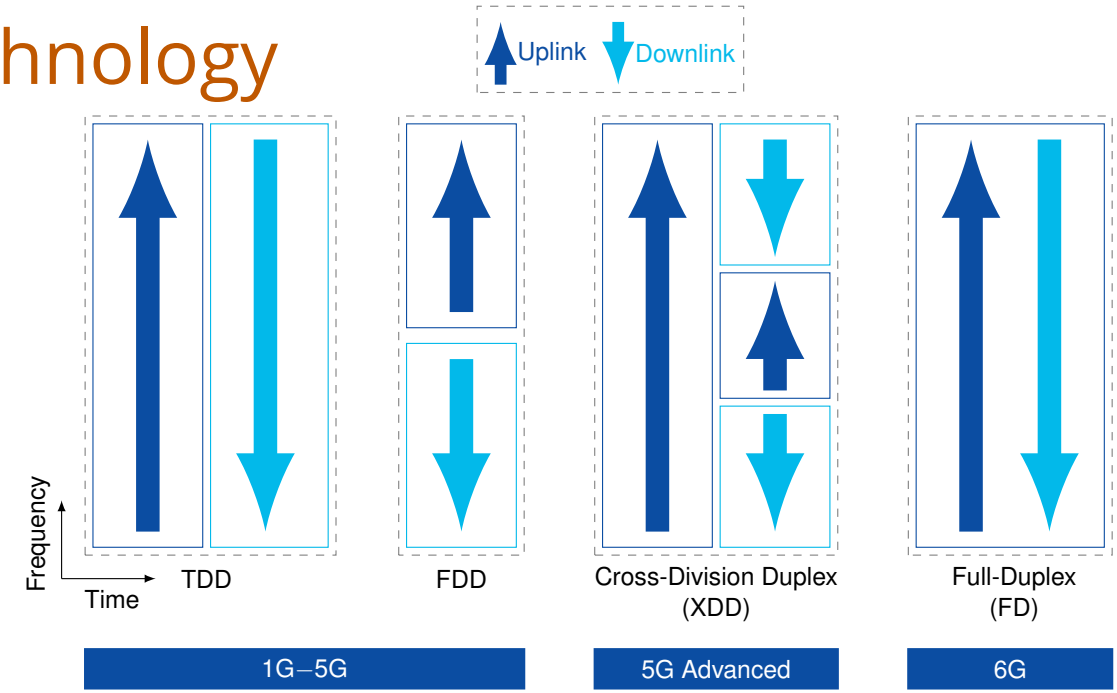

Evolution of duplex technology with Cross Division Duplexing (XDD) and Full-Duplex (FD)

- In Frequency Division Duplexing (FDD) and Time Division Duplexing (TDD), downlink and uplink signals are transmitted in a “mutually exclusive" way
- Uplink issues in Time Division Duplexing: short transmission period affects coverage (longer distance times out faster) and data rate (switching overhead)
- Cross Division Duplexing can increase uplink communication coverage and reduce latency by enabling long uplink transmission
- Full Duplex can increase capacity (max 2x in theory), reduce latency, and improve uplink coverage by deviating from the “mutually exclusive" principle

H. Ji, Y. Kim, K. Muhammad, C. Tarver, M. Tonnemacher, T. Kim, J. Oh, B. Yu, G. Xu, and J. Lee. Extending 5G TDD Coverage With XDD: Cross Division Duplex. In: *IEEE Access* 9 (2021), pp. 51380–51392.

Full-Duplex Challenges

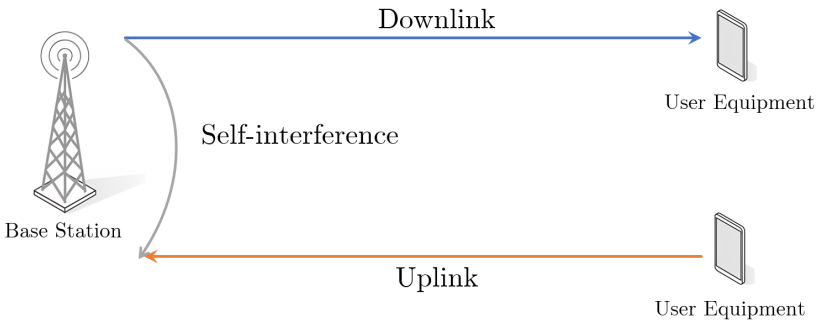

(a) Self-interference

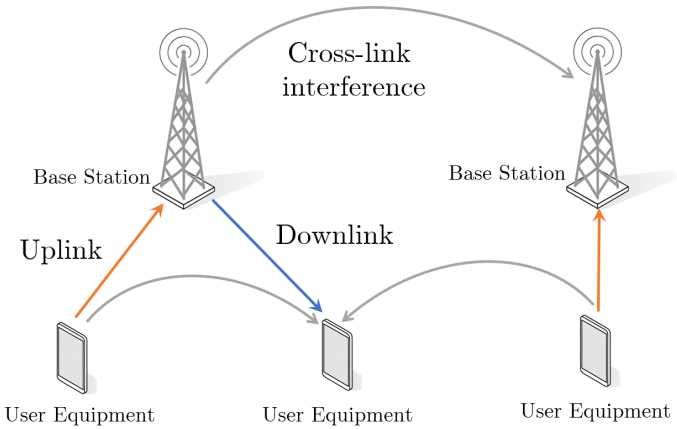

(b) Cross-link interference

- Near-far problem (left): collocated transmit/receive arrays of full-duplex basestation receiving from far uplink user
  - Incurs self-interference (100-160 dB) higher than uplink received power
  - Self-interference more severe for cell-edge users due to high pathloss
  - Saturates receiver analog-to-digital converters (ADCs) reducing data rate
- Cross-link interference (right): inter-user and basestation-to-basestation interference

Contributions

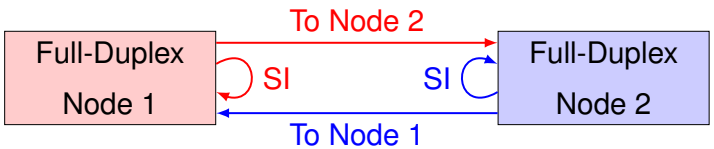

Contribution 1: Point-to-Point System

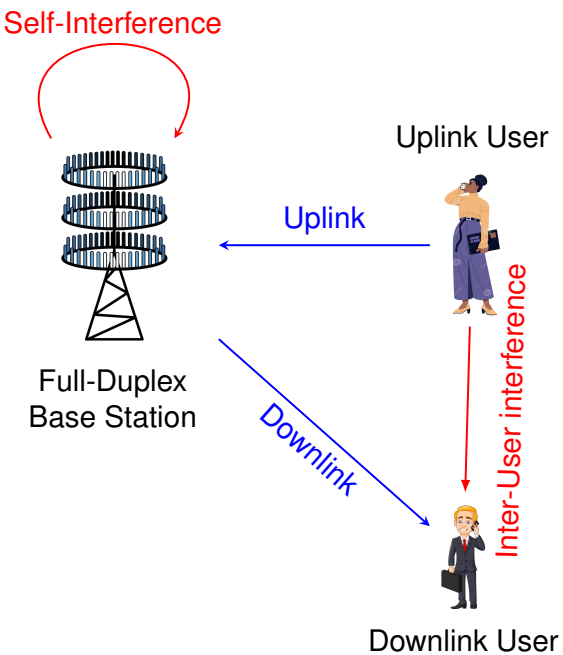

Contribution 2: Single-Cell Single-User MIMO

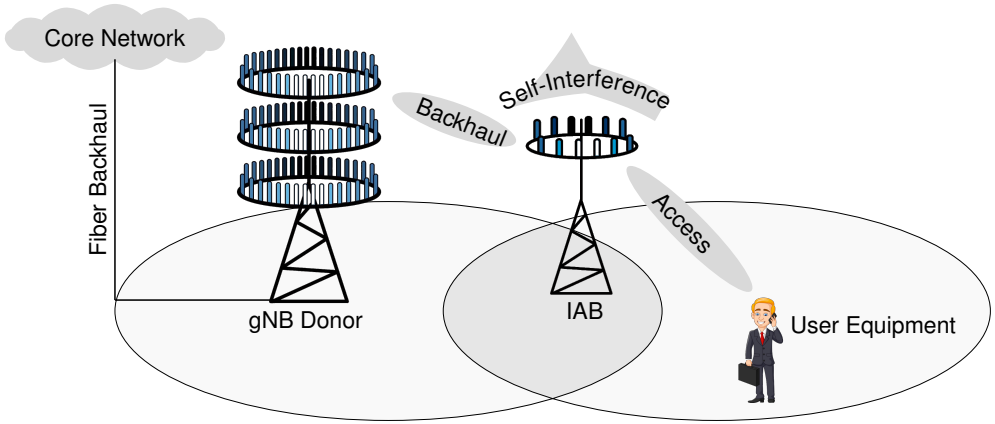

Contribution 3: Integrated Access and Backhaul

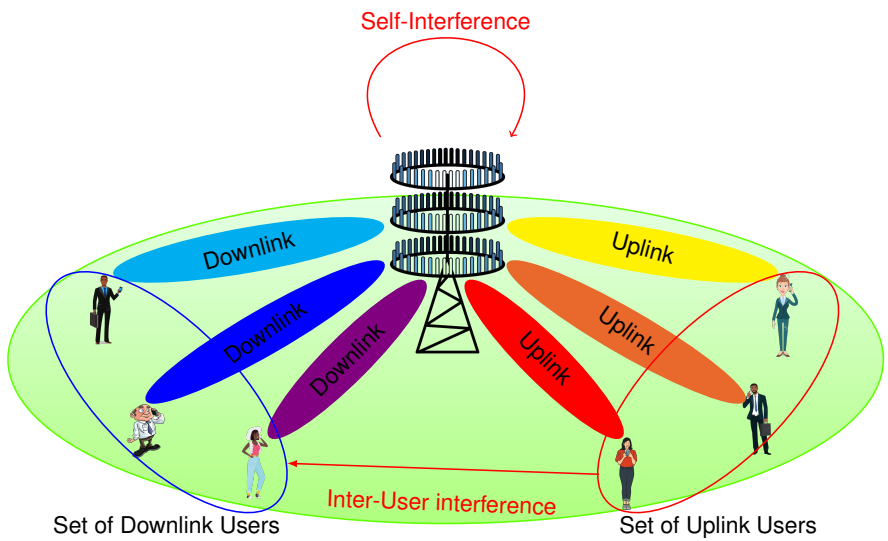

Contribution 4: Single-Cell Multiuser MIMO

Contributions

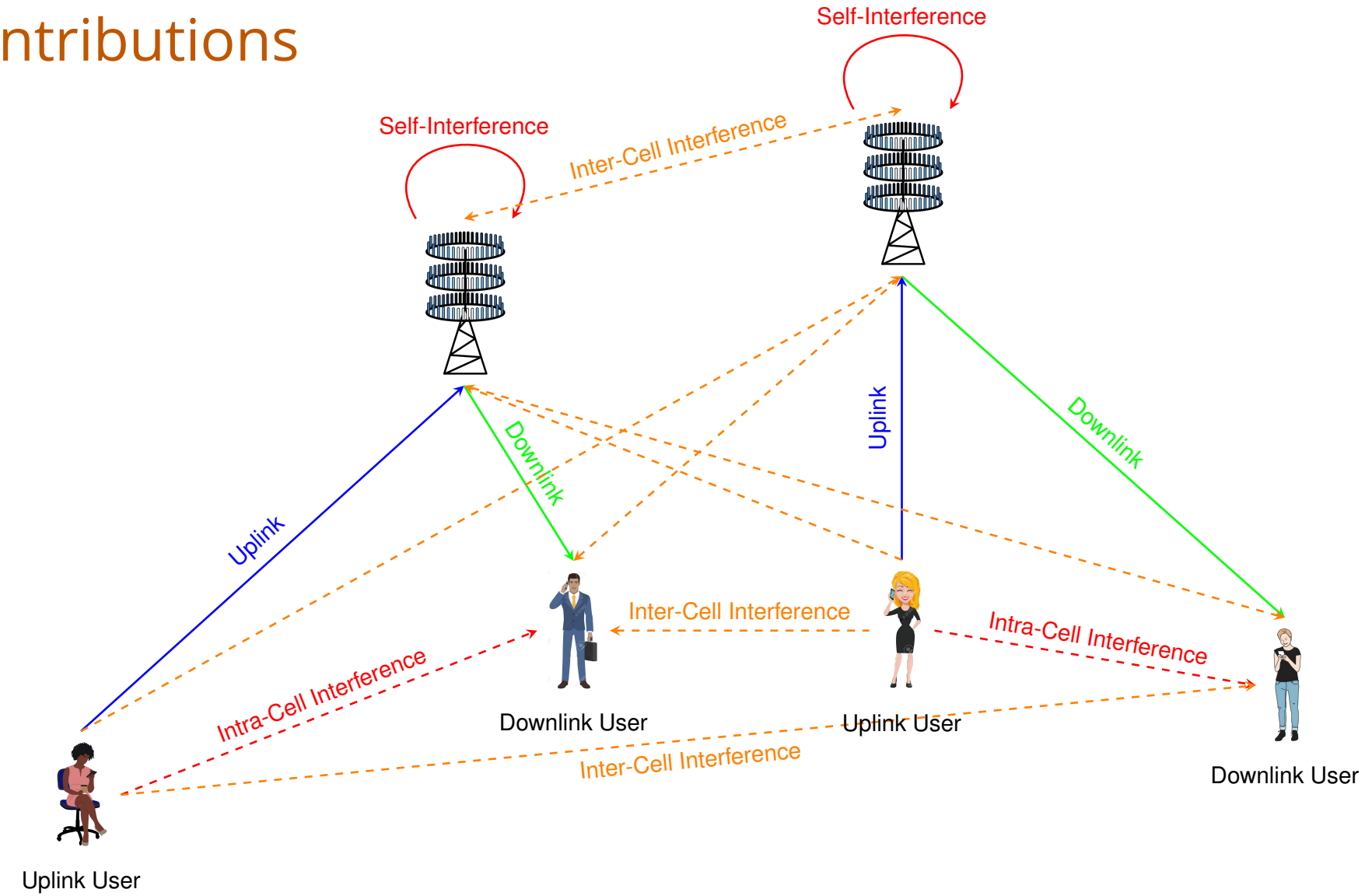

Contribution 5: Multi-Cell Multiuser MIMO (Cellular Networks)

Contributions

- Use the degrees of freedom in large-antenna full-duplex cellular systems to suppress self-interference and increase data rates
  - Design low-complex and robust hybrid analog/digital beamformers against SI
  - Achieve large SI reduction in the analog domain to avoid ADC saturation
  - Prove feasibility of FD cellular systems

Contributions

1. Point-to-Point System
2. Single-Cell Single-User MIMO
3. Integrated Access and Backhaul
4. Single-Cell Multiuser MIMO
5. Multicell Multiuser MIMO (cellular networks)

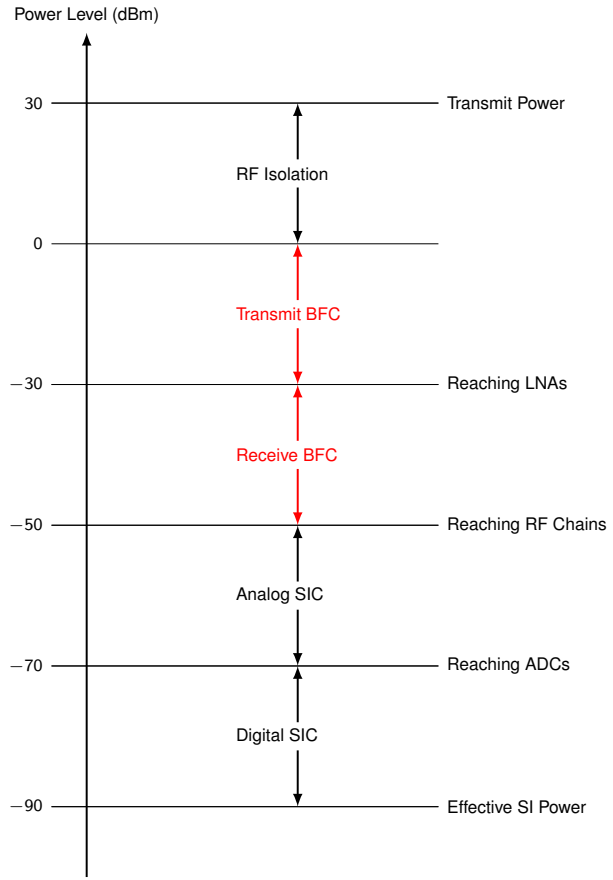

Example breakdown of successive interference cancellation (SIC) power levels at various points in a full duplex mmWave transceiver employing beamforming cancellation (BFC)

Ian P. Roberts, Jeffrey G. Andrews, Hardik B. Jain, and Sriram Vishwanath. Millimeter-Wave Full Duplex Radios: New Challenges and Techniques. In: *IEEE Wireless Communications* 28.1 (2021), pp. 36–43.

Outline

Description

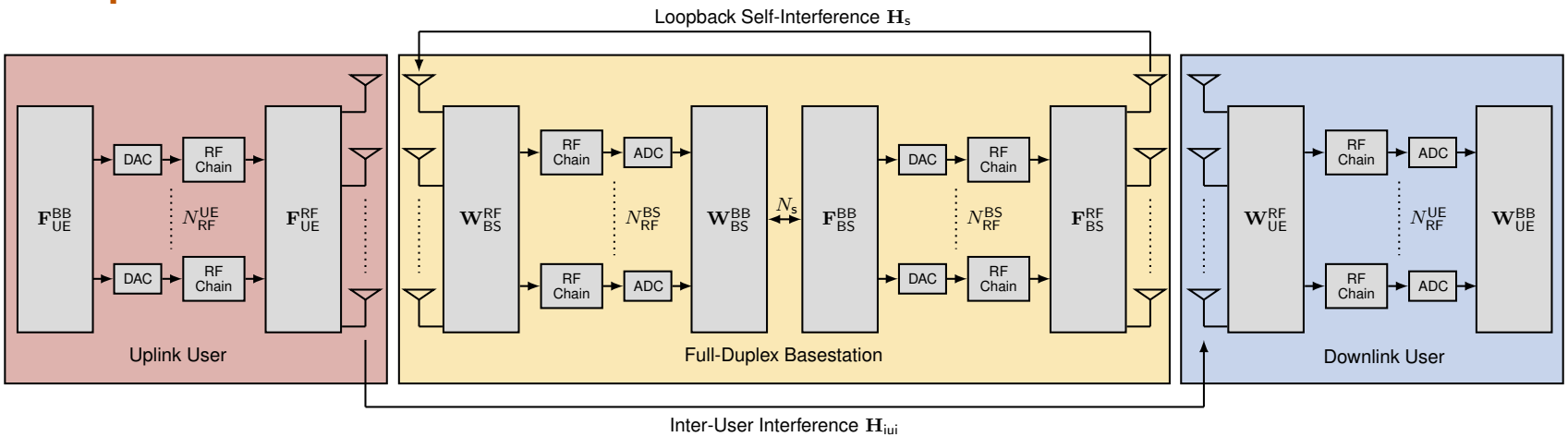

Hybrid analog/digital beamforming architecture of a single-user MIMO system

- FD base station (BS) simultaneously communicates with uplink and downlink users in the same resource block
- Hybrid beamformers decomposed into analog (RF) and baseband (BB) modules
- Uplink user is corrupted by loopback SI
- Downlink user is disrupted by inter-user interference (IUI) incurred by uplink user
- Analog beamformers at users and BS: $\mathbf{F}_{UE}^{RF}$, $\mathbf{W}_{UE}^{RF}$, $\mathbf{F}_{BS}^{RF}$ and $\mathbf{W}_{BS}^{RF}$
- Baseband beamformers at users and BS: $\mathbf{F}_{UE}^{BB}$, $\mathbf{W}_{UE}^{BB}$, $\mathbf{F}_{BS}^{BB}$ and $\mathbf{W}_{BS}^{BB}$

Elyes Balti, Salam Akoum, Iyad Alfalujah, and Brian L. Evans. Hybrid Beamforming Design for Full-Duplex Millimeter Wave Massive MIMO Systems. In: *IEEE Transactions on Vehicular Technology* 73.11 (2024), pp. 17041–17058.

Signal Model

- The uplink received signal $\left(y_u \in \mathbb{C}^{N_s \times 1}\right)$ at the base station is

$$y_u = \underbrace{\sqrt{\rho_u} W_{BS}^{BB*} W_{BS}^{RF*} H_u F_{UE}^{RF} F_{UE}^{BB} s_u}_{\text{Desired Signal}} + \underbrace{\sqrt{\rho_s} W_{BS}^{BB*} W_{BS}^{RF*} H_s F_{BS}^{RF} F_{BS}^{BB} s_d}_{\text{Self-Interference Signal}} + \underbrace{W_{BS}^{BB*} W_{BS}^{RF*} n_{BS}}_{\text{Filtered Noise}} \quad (1)$$

- The downlink received signal $\left(y_d \in \mathbb{C}^{N_s \times 1}\right)$ at the UE is expressed by

$$y_d = \underbrace{\sqrt{\rho_d} W_{UE}^{BB*} W_{UE}^{RF*} H_d F_{BS}^{RF} F_{BS}^{BB} s_d}_{\text{Desired Signal}} + \underbrace{\sqrt{\rho_{iui}} W_{UE}^{BB*} W_{UE}^{RF*} H_{iui} F_{UE}^{RF} F_{UE}^{BB} s_u}_{\text{Inter-User Interference Signal}} + \underbrace{W_{UE}^{BB*} W_{UE}^{RF*} n_{UE}}_{\text{Filtered Noise}} \quad (2)$$

- s_u and s_d are the uplink and downlink transmit symbols, respectively.
- ρ_u, ρ_d, ρ_s and ρ_{iui} are the large-scale average received uplink, downlink, SI and IUI powers, respectively
- H_u, H_d, H_s and H_{iui} are the uplink, downlink, SI and IUI channels, respectively.
- n_{BS} and n_{UE} are the AWGN at the BS and UE, respectively

Hybrid Analog/Baseband Problem Formulation

- To maximize the sum uplink/downlink spectral efficiency

$$
\begin{aligned}
\mathscr{P}_1 : \quad & \max_{\substack{\mathbf{W}_{\mathbf{BS}}^{\mathbf{RF}},\mathbf{F}_{\mathbf{BS}}^{\mathbf{RF}},\mathbf{W}_{\mathbf{UE}}^{\mathbf{RF}},\mathbf{F}_{\mathbf{UE}}^{\mathbf{RF}} \\ \mathbf{W}_{\mathbf{BS}}^{\mathbf{BB}},\mathbf{F}_{\mathbf{BS}}^{\mathbf{BB}},\mathbf{W}_{\mathbf{UE}}^{\mathbf{BB}},\mathbf{F}_{\mathbf{UE}}^{\mathbf{BB}}}} \mathcal{I}_{\mathbf{u}} + \mathcal{I}_{\mathbf{d}} \\
\text{s.t.} \quad & \|\mathbf{F}_{\mathrm{BS}}^{\mathrm{RF}}\mathbf{F}_{\mathrm{BS}}^{\mathrm{BB}}\|_F^2 = N_{\mathbf{s}} \ (\textit{Downlink transmit power}) \\
& \|\mathbf{F}_{\mathrm{UE}}^{\mathrm{RF}}\mathbf{F}_{\mathrm{UE}}^{\mathrm{BB}}\|_F^2 = N_{\mathbf{s}} \ (\textit{Uplink transmit power}) \\
& \mathbf{F}_{\mathrm{BS}}^{\mathrm{RF}}, \mathbf{F}_{\mathrm{UE}}^{\mathrm{RF}} \in \mathcal{F}_{\mathrm{RF}} \ (\textit{Unit} - \textit{modulus}, \textit{set of feasible RF precoders}) \\
& \mathbf{W}_{\mathrm{BS}}^{\mathrm{RF}}, \mathbf{W}_{\mathrm{UE}}^{\mathrm{RF}} \in \mathcal{W}_{\mathrm{RF}} \ (\textit{Unit} - \textit{modulus}, \textit{set of feasible RF combiners}) \\
& \mathbf{W}_{\mathrm{BS}}^{\mathrm{RF}*}\mathbf{H}_{\mathbf{s}}\mathbf{F}_{\mathrm{BS}}^{\mathrm{RF}} = 0 \ (\textit{Self} - \textit{interference suppression}) \\
& \mathbf{W}_{\mathrm{UE}}^{\mathrm{RF}*}\mathbf{H}_{\mathbf{iui}}\mathbf{F}_{\mathrm{UE}}^{\mathrm{RF}} = 0 \ (\textit{Inter} - \textit{user interference suppression})
\end{aligned}
\tag{3}
$$

- Decompose the hybrid beamforming problem into two stages: Analog and baseband

Analog Beamforming Stage

- The analog beamforming problem is stated as

$$
\begin{aligned}
\mathscr{P}_2 : \max_{W_{BS}^{RF}, F_{BS}^{RF}, W_{UE}^{RF}, F_{UE}^{RF}} \; & \mathcal{I}_u + \mathcal{I}_d \\
\text{s.t. } & F_{BS}^{RF}, F_{UE}^{RF} \in \mathcal{F}_{RF} \; (\textit{Unit} - \textit{modulus}, \textit{set of feasible RF precoders}) \\
& W_{BS}^{RF}, W_{UE}^{RF} \in \mathcal{W}_{RF} \; (\textit{Unit} - \textit{modulus}, \textit{set of feasible RF combiners}) \\
& W_{BS}^{RF*} \underbrace{H_s F_{BS}^{RF}}_{=C} = 0 \; (\textit{Self} - \textit{interference suppression}) \\
& W_{UE}^{RF*} H_{iui} F_{UE}^{RF} = 0 \; (\textit{Inter} - \textit{user interference suppression})
\end{aligned} \tag{4}
$$

- A preliminary solution (W_{BS}^{RF}) is given by
  1. Maximize the received power by taking the N_{RF}^{BS} dominant left singular vectors of the uplink beamformed channel $H_u F_{UE}^{RF} F_{UE}^{BB}$
  2. Suppress the effective SI by projecting the BS analog combiner on the SI null-space ($P_\perp = I - CC^\dagger$)
  3. Project the BS analog combiner onto the unit modulus space ($\mathcal{W}_{RF}$)
- Limitation: The projection onto the unit modulus space (2) violates the interference suppression constraint (3)

Analog Beamforming Solution

- Seek for the optimal subspace that minimizes the loss
- *Alternating Projection* Method: Successive projections between interference-null space and unit-modulus space until convergence

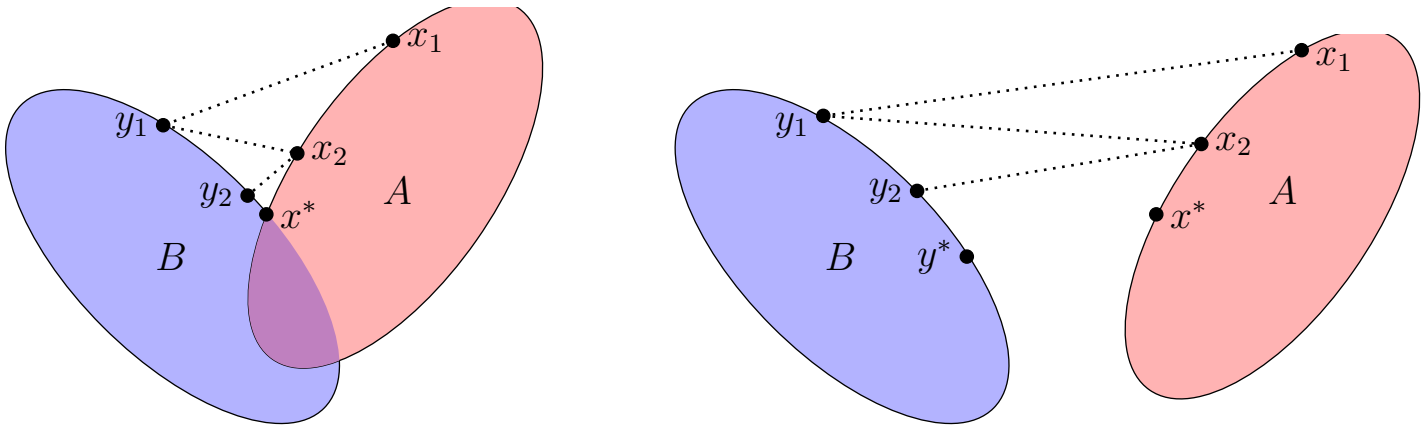

(a) $A \cap B \neq \emptyset$ (b) $A \cap B = \emptyset$

First few iterations of the Alternating Projections Method. (a) Both sequences are converging to the point $x^* \in A \cap B$. (b) Sequence x_k is converging to $x^* \in A$, and the sequence y_k is converging to $y^* \in B$, where $\|x^* - y^*\|_2 = \mathbf{dist(A, B)}$

- Fix the solution (W_{BS}^{RF}) and repeat the same routine to solve for (F_{BS}^{RF}), (F_{UE}^{RF}) and (W_{UE}^{RF})

Baseband Beamforming Solution

- The baseband beamformers are solved using Least Squares routine as

$$W_{BS}^{BB} = W_{BS}^{RF\dagger} W_{BS} \quad (5)$$

$$F_{BS}^{BB} = F_{BS}^{RF\dagger} F_{BS} \quad (6)$$

$$W_{UE}^{BB} = W_{UE}^{RF\dagger} W_{UE} \quad (7)$$

$$F_{UE}^{BB} = F_{UE}^{RF\dagger} F_{UE} \quad (8)$$

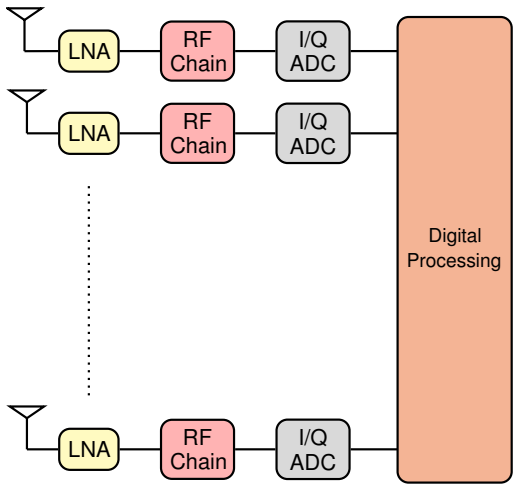

All-digital combiner

- To satisfy the transmit power constraint in (3), we normalize the digital precoders at BS and UE by a factor of $\frac{\sqrt{N_s}}{\|F_{BS}^{RF} F_{BS}^{BB}\|_F}$ and $\frac{\sqrt{N_s}}{\|F_{UE}^{RF} F_{UE}^{BB}\|_F}$
- Note that W_{BS}, F_{BS}, W_{UE} and F_{UE} are the all-digital beamformers
- All-digital architecture achieves the best spectral efficiency, however, it consumes a prohibitively large amount of power. NOT practical
- All-digital beamformers are derived to serve as a benchmark
- The analog and baseband beamformers are coupled. Hence, an iterative routine is carried out until convergence

Complexity and Convergence

Algorithm 2 Hybrid Beamforming Design

function ANALOG($\mathbf{A}, \mathbf{C}, L$)
  $\mathbf{X}_{\mathsf{RF}} \leftarrow L$ Dominant left singular vectors of $\mathbf{A}$
  $\mathbf{P}_{\perp} \leftarrow \mathbf{I} - \mathbf{C}\mathbf{C}^{*}$ (Interference null-space matrix)
  Set $n = 0$
  repeat (Inner loop for alternating projections)
    $\mathbf{X}_{\mathsf{RF}}^{(n+1)} \leftarrow \mathbf{P}_{\perp}\mathbf{X}_{\mathsf{RF}}^{(n)}$
    for $i \leftarrow 1 : M$ and $j \leftarrow 1 : L$ **do**
      $\left(\mathbf{X}_{\mathsf{RF}}^{(n)}\right)_{ij} \leftarrow \left(\mathbf{X}_{\mathsf{RF}}^{(n+1)}\right)_{ij} / \left|\left(\mathbf{X}_{\mathsf{RF}}^{(n+1)}\right)_{ij}\right|$
    end for
    $n \leftarrow n + 1$
  until Convergence
  return $\mathbf{X}_{\mathsf{RF}} \in \mathbb{C}^{M \times L}$
end function

Input $\mathbf{H}_{\mathsf{u}}$, $\mathbf{H}_{\mathsf{d}}$, $\mathbf{H}_{\mathsf{s}}$ and $\mathbf{H}_{\mathsf{iui}}$
Initialize $\mathbf{F}_{\mathsf{UE}}^{\mathsf{RF}}$, $\mathbf{F}_{\mathsf{UE}}^{\mathsf{BB}}$, $\mathbf{W}_{\mathsf{UE}}^{\mathsf{RF}}$, $\mathbf{W}_{\mathsf{UE}}^{\mathsf{BB}}$ and $\mathbf{F}_{\mathsf{BS}}^{\mathsf{RF}}$
Obtain $\mathbf{W}_{\mathsf{BS}}, \mathbf{F}_{\mathsf{BS}}, \mathbf{W}_{\mathsf{UE}}$ and $\mathbf{F}_{\mathsf{UE}}$ from Algorithm 1
Set $k = 0$
repeat (Outer loop)
  $\mathbf{W}_{\mathsf{BS}}^{\mathsf{RF}(k+1)} \leftarrow$
  $\text{ANALOG}(\mathbf{H}_{\mathsf{u}}\mathbf{F}_{\mathsf{UE}}^{\mathsf{RF}(k)}\mathbf{F}_{\mathsf{UE}}^{\mathsf{BB}(k)}, \mathbf{H}_{\mathsf{s}}\mathbf{F}_{\mathsf{BS}}^{\mathsf{RF}(k)}, N_{\mathsf{RF}}^{\mathsf{BS}})$
  $\mathbf{W}_{\mathsf{BS}}^{\mathsf{BB}(k+1)} \leftarrow \mathbf{W}_{\mathsf{BS}}^{\mathsf{RF}(k+1)\dagger}\mathbf{W}_{\mathsf{BS}}$ (LS Solution)
  $\mathbf{F}_{\mathsf{BS}}^{\mathsf{RF}(k+1)} \leftarrow$
  $\text{ANALOG}(\mathbf{H}_{\mathsf{d}}^{*}\mathbf{W}_{\mathsf{UE}}^{\mathsf{RF}(k)}\mathbf{W}_{\mathsf{UE}}^{\mathsf{BB}(k)}, \mathbf{H}_{\mathsf{s}}^{*}\mathbf{W}_{\mathsf{BS}}^{\mathsf{RF}(k+1)}, N_{\mathsf{RF}}^{\mathsf{BS}})$
  $\mathbf{F}_{\mathsf{BS}}^{\mathsf{BB}(k+1)} \leftarrow \mathbf{F}_{\mathsf{BS}}^{\mathsf{RF}(k+1)\dagger}\mathbf{F}_{\mathsf{BS}}$
  $\mathbf{W}_{\mathsf{UE}}^{\mathsf{RF}(k+1)} \leftarrow$
  $\text{ANALOG}(\mathbf{H}_{\mathsf{d}}\mathbf{F}_{\mathsf{BS}}^{\mathsf{RF}(k+1)}\mathbf{F}_{\mathsf{BS}}^{\mathsf{BB}(k+1)}, \mathbf{H}_{\mathsf{iui}}\mathbf{F}_{\mathsf{UE}}^{\mathsf{RF}(k)}, N_{\mathsf{RF}}^{\mathsf{UE}})$
  $\mathbf{W}_{\mathsf{UE}}^{\mathsf{BB}(k+1)} \leftarrow \mathbf{W}_{\mathsf{UE}}^{\mathsf{RF}(k+1)\dagger}\mathbf{W}_{\mathsf{UE}}$
  $\mathbf{F}_{\mathsf{UE}}^{\mathsf{RF}(k+1)} \leftarrow$
  $\text{ANALOG}(\mathbf{H}_{\mathsf{u}}^{*}\mathbf{W}_{\mathsf{BS}}^{\mathsf{RF}(k+1)}\mathbf{W}_{\mathsf{BS}}^{\mathsf{BB}(k+1)}, \mathbf{H}_{\mathsf{iui}}^{*}\mathbf{W}_{\mathsf{UE}}^{\mathsf{RF}(k+1)}, N_{\mathsf{RF}}^{\mathsf{UE}})$
  $\mathbf{F}_{\mathsf{UE}}^{\mathsf{BB}(k+1)} \leftarrow \mathbf{F}_{\mathsf{UE}}^{\mathsf{RF}(k+1)\dagger}\mathbf{F}_{\mathsf{UE}}$
  $k \leftarrow k + 1$
until Convergence
Normalize the digital precoders at BS and UE as $\mathbf{F}_{\mathsf{BS}}^{\mathsf{BB}} \leftarrow \frac{\sqrt{N_{\mathsf{s}}}}{\|\mathbf{F}_{\mathsf{BS}}^{\mathsf{RF}}\mathbf{F}_{\mathsf{BS}}^{\mathsf{BB}}\|_F}\mathbf{F}_{\mathsf{BS}}^{\mathsf{BB}}$, $\mathbf{F}_{\mathsf{UE}}^{\mathsf{BB}} \leftarrow \frac{\sqrt{N_{\mathsf{s}}}}{\|\mathbf{F}_{\mathsf{UE}}^{\mathsf{RF}}\mathbf{F}_{\mathsf{UE}}^{\mathsf{BB}}\|_F}\mathbf{F}_{\mathsf{UE}}^{\mathsf{BB}}$
return $\mathbf{W}_{\mathsf{BS}}^{\mathsf{RF}}, \mathbf{W}_{\mathsf{BS}}^{\mathsf{BB}}, \mathbf{F}_{\mathsf{BS}}^{\mathsf{RF}}, \mathbf{F}_{\mathsf{BS}}^{\mathsf{BB}}, \mathbf{W}_{\mathsf{UE}}^{\mathsf{RF}}, \mathbf{W}_{\mathsf{UE}}^{\mathsf{BB}}, \mathbf{F}_{\mathsf{UE}}^{\mathsf{RF}}, \mathbf{F}_{\mathsf{UE}}^{\mathsf{BB}}$

Table 1: Complexity Analysis

Beamformer	Cost
$\mathsf{W}_{\mathsf{BS}}, \mathsf{F}_{\mathsf{BS}}$	$\mathcal{O}(N_{\mathsf{BS}}^3)$
$\mathsf{W}_{\mathsf{UE}}, \mathsf{F}_{\mathsf{UE}}$	$\mathcal{O}(N_{\mathsf{UE}}^3)$
$\mathsf{W}_{\mathsf{BS}}^{\mathsf{RF}}, \mathsf{F}_{\mathsf{BS}}^{\mathsf{RF}}$	$\mathcal{O}\left(N_{\mathsf{inner}}(N_{\mathsf{UE}}N_{\mathsf{s}}^2 + 2N_{\mathsf{BS}}^2 N_{\mathsf{RF}}^{\mathsf{BS}})\right)$
$\mathsf{W}_{\mathsf{UE}}^{\mathsf{RF}}, \mathsf{F}_{\mathsf{UE}}^{\mathsf{RF}}$	$\mathcal{O}\left(N_{\mathsf{inner}}(N_{\mathsf{BS}}N_{\mathsf{s}}^2 + 2N_{\mathsf{UE}}^2 N_{\mathsf{RF}}^{\mathsf{UE}})\right)$
$\mathsf{W}_{\mathsf{BS}}^{\mathsf{BB}}, \mathsf{F}_{\mathsf{BS}}^{\mathsf{BB}}$	$\mathcal{O}(N_{\mathsf{BS}}(N_{\mathsf{BS}}^{\mathsf{RF}})^2 + N_{\mathsf{BS}}^{\mathsf{RF}}N_{\mathsf{BS}}N_{\mathsf{s}})$
$\mathsf{W}_{\mathsf{UE}}^{\mathsf{BB}}, \mathsf{F}_{\mathsf{UE}}^{\mathsf{BB}}$	$\mathcal{O}(N_{\mathsf{UE}}(N_{\mathsf{UE}}^{\mathsf{RF}})^2 + N_{\mathsf{UE}}^{\mathsf{RF}}N_{\mathsf{UE}}N_{\mathsf{s}})$

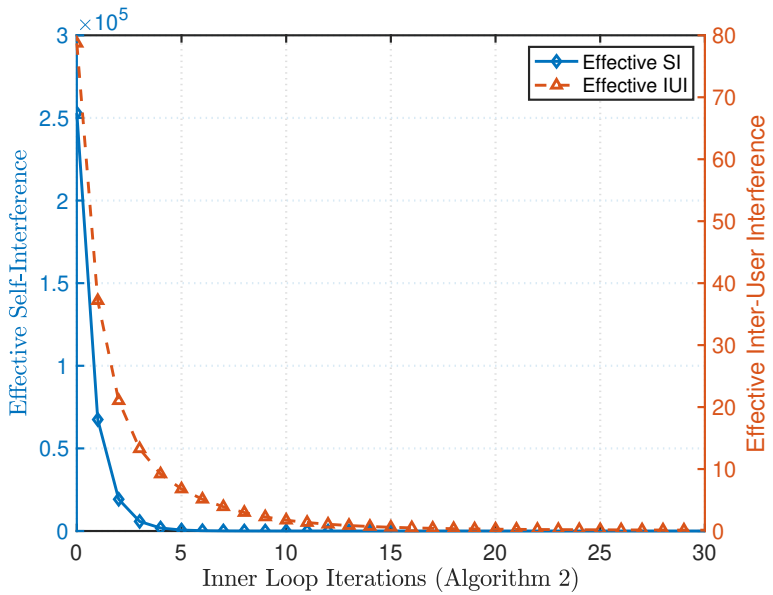

Effect of the Inner Loop Iterations: Convergence of Alternating Projections Method

Bounds

- Singular Value Decomposition (SVD): Assuming no interference ($\rho_s = \rho_{iui} = 0$) and neglecting hardware constraints, so that W_{BS}, F_{BS}, W_{UE}, F_{UE} are only constrained to be semi-unitary matrices

$$\mathcal{I}_{\text{Bound}} = \sum_{\ell=0}^{N_s-1} \log\left(1+\sigma_\ell\left(H_u\right)^2 \text{SNR}\right) + \sum_{\ell=0}^{N_s-1} \log\left(1+\sigma_\ell\left(H_d\right)^2 \text{SNR}\right) \tag{9}$$

  where $\sigma_\ell(H)$ is the ℓ-th singular value of X in descending order
- SVD with Waterfilling: With the optimum beamformers diagonalizing the channel $H \in \mathbb{C}^{N_r \times N_t}$ and allocating power via waterfilling, the capacity bound equals

$$\mathcal{I}_{\text{WF}} = \sum_{\ell=0}^{N_{\text{min}}-1} \left[\log\left(\frac{\text{SNR}}{N_t}\frac{\lambda_\ell\left(H^*H\right)}{\eta}\right)\right]^+ \tag{10}$$

  where $N_{\text{min}} = \min(N_t, N_r) \geq N_s$, and the optimized power per ℓ-th stream is given by

$$P_\ell^\star = \left[\frac{1}{\eta} - \frac{N_t}{\text{SNR}\lambda_\ell\left(H^*H\right)}\right]^+, \quad \ell = 0, \ldots, N_{\text{min}}-1, \tag{11}$$

  Note that η must satisfy that $\sum_\ell P_\ell^\star = P_{\text{total}}$, and $\lambda_\ell(X)$ is the ℓ-th eigenvalue of X in descending order and $[x]^+ = \max(0, x)$

Numerical Results

Table 2: Simulation Parameters (Narrowband)

Parameter	**Value**
Carrier Frequency	28 GHz
Bandwidth (B)	1 GHz
Number of BS Antennas (N_{BS})	16, 32, 64, 128, 256, 512
Number of UE Antennas (N_{UE})	4, 8
Number of Spatial Streams (N_{s})	1, 2
Number of RF Chains at BS ($N_{\mathrm{RF}}^{\mathrm{BS}}$)	1, 2, 4, 8, 16, 32, 64, 128
Number of RF Chains at UE ($N_{\mathrm{RF}}^{\mathrm{UE}}$)	1, 2, 4
Number of Clusters (C)	6
Number of Rays per Cluster (R_c)	8
AoA/AoD Angular Spread	20°
Transceivers Gap (d)	2λ
Transceivers Incline (ω)	$\frac{\pi}{6}$
Rician Factor (κ)	5 dB
Average Receive SI Power (ρ_{s})	15, 30 dB
Average Receive IUI Power (ρ_{iui})	5 dB

Self-Interference, Spectral Efficiency and SINR

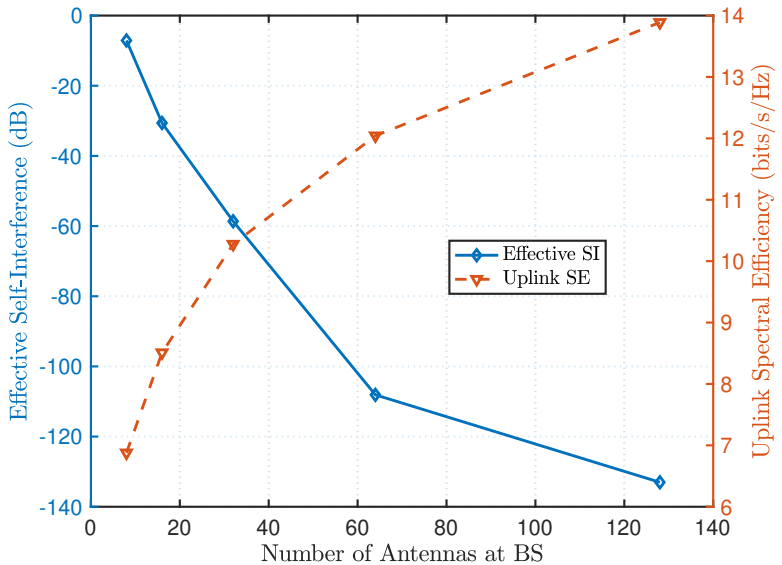

(a)

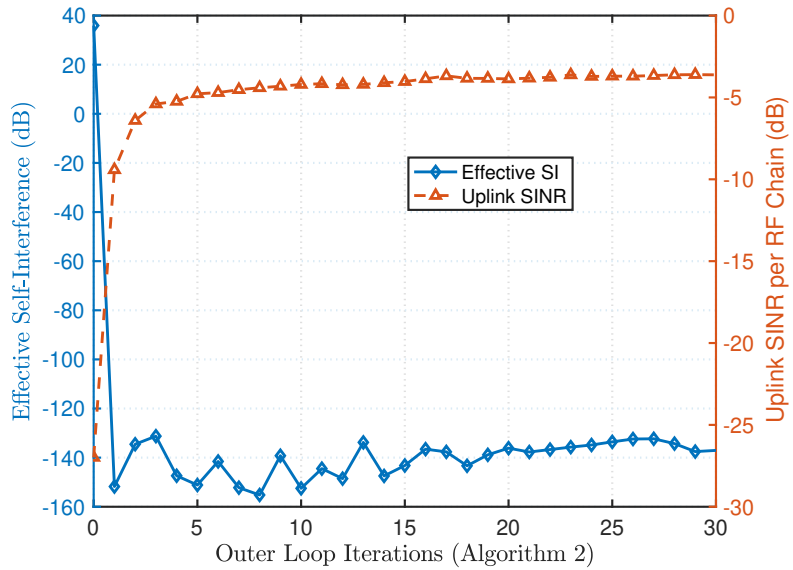

(b)

(a) Effect of the number of antennas on self-interference and uplink data rate. (b) Convergence of the proposed algorithm measured in interference power and uplink signal-to-interference-plus-noise ratio (SINR)

- (Left) Degrees of freedom balanced between suppressing interference and increasing data rate
- (Left) Increasing number of antennas from 4 to 128 reduces self-interference by about 120 dB and doubles the data rate from 6.7 to 14 bits/s/Hz
- (Right) Fast convergence (3-5 iterations) in log-scale
- (Right) Reduces self-interference by 180 dB and increases SINR by 25 dB

Spectral Efficiency

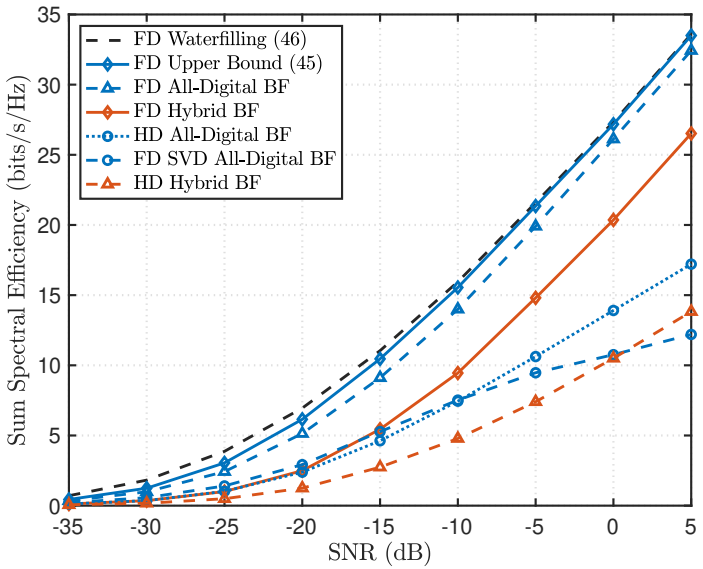

(a)

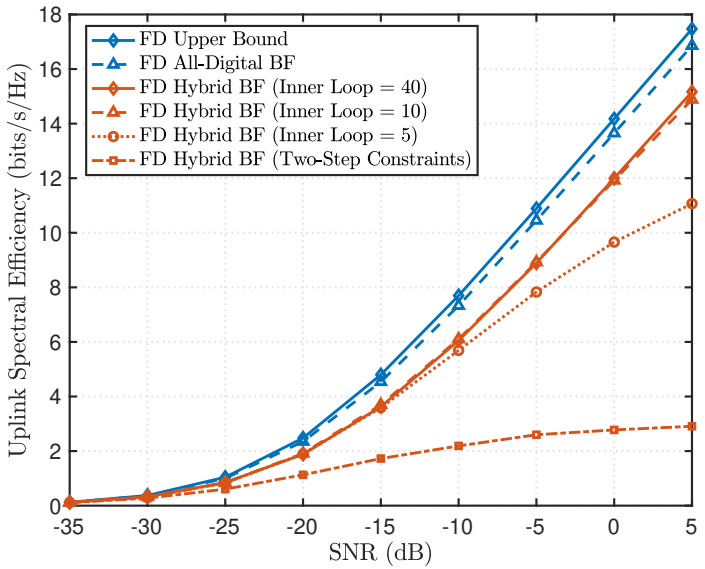

(b)

(a) Sum uplink/downlink data rate vs. half-duplex. (b) uplink data rate vs. inner loop

- Gap with all-digital: reduction in RF chains + unit modulus constraint (steering the beams only using the phase shifters; phased arrays)
- Our hybrid FD design outperforms the half-duplex (hybrid and all-digital)
- Previous approaches saturated by interference, since unit modulus violates the interference suppression constraint
- Alternating projections (inner loop) minimizes the loss incurred by the two concurrent constraints (unit-modulus and interference suppression)

Outline

System Model

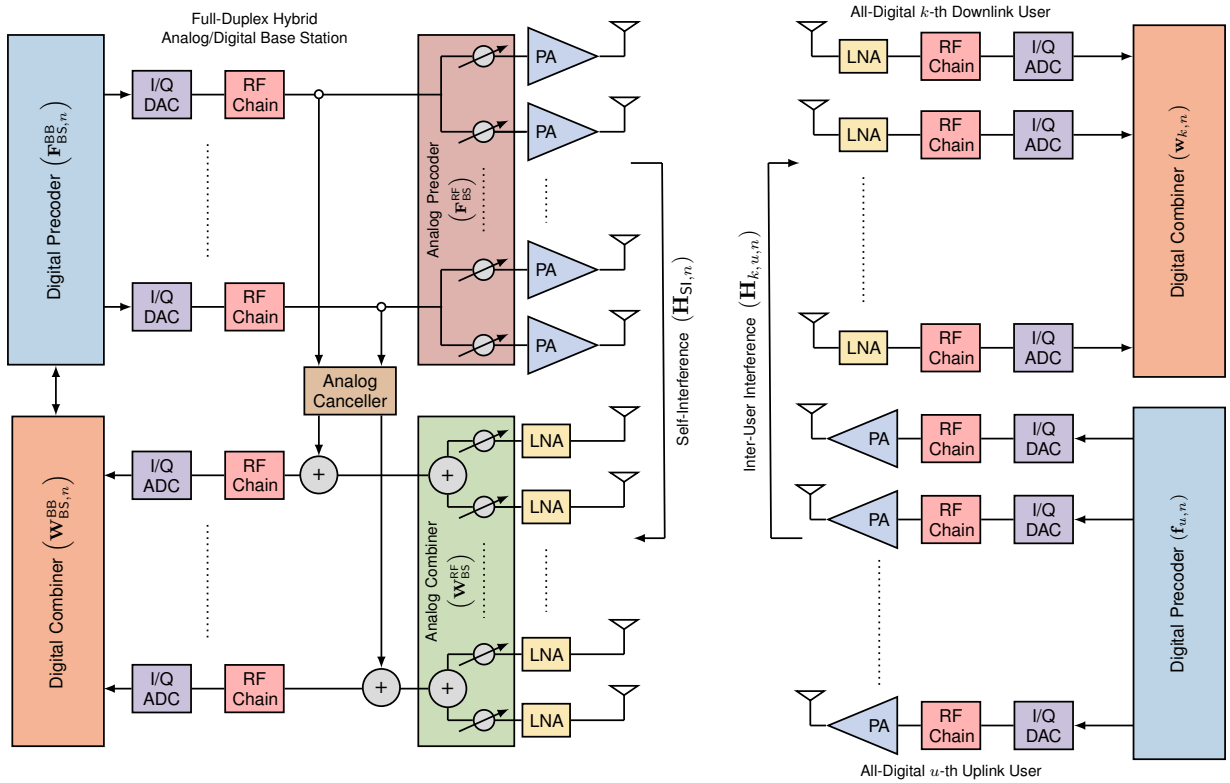

Hybrid analog/digital architecture of the full-duplex base station and the all-digital structure of the users

- Full-duplex base station simultaneously communicates with uplink and downlink users in the same resource (time/frequency) block
- Uplink users are corrupted by loopback self-interference
- Downlink users are vulnerable to inter-user interference from uplink users
- Partially connected array at the BS with quantized phase shifters

Signal Model

- The u-th uplink received signal at the BS for subcarrier n is

$$y_{u,n} = \underbrace{w_{BS,u,n}^{BB*} W_{BS}^{RF*} H_{u,n} f_{u,n} x_{u,n}}_{\text{Desired Signal}} + \underbrace{w_{BS,u,n}^{BB*} W_{BS}^{RF*} n_{BS,n}}_{\text{Filtered Noise}}$$
$$+ \underbrace{w_{BS,u,n}^{BB*} W_{BS}^{RF*} H_{SI,n} F_{BS}^{RF} F_{BS,n}^{BB} x_{BS,n}}_{\text{Self-Interference (SI)}} + \underbrace{w_{BS,u,n}^{BB*} W_{BS}^{RF*} \sum_{u \neq u}^{U-1} H_{u,n} f_{u,n} x_{u,n}}_{\text{Multiuser Interference (MUI)}} \tag{12}$$

- The received signal at the k-th downlink user and at the n-th subcarrier is

$$y_{k,n} = \underbrace{w_{k,n}^{*} H_{k,n} F_{BS}^{RF} f_{BS,k,n}^{BB} x_{BS,k,n}}_{\text{Desired Signal}} + \underbrace{w_{k,n}^{*} \sum_{u=0}^{U-1} H_{k,u,n} f_{u,n} x_{u,n}}_{\text{Inter-User Interference (IUI)}}$$
$$+ \underbrace{w_{k,n}^{*} \sum_{k \neq k}^{K-1} H_{k,n} F_{BS}^{RF} f_{BS,k,n}^{BB} x_{BS,k,n}}_{\text{Multiuser Interference (MUI)}} + \underbrace{w_{k,n}^{*} n_{UE,n}}_{\text{Filtered Noise}} \tag{13}$$

- Objective: Design the four beamforming matrices (in burnt orange) at the BS

Analog Beamforming

- The SI level before the ADC is

$$\mathbf{C}_{\mathbf{SI},n} = \mathbf{W}_{\mathbf{BS}}^{\mathbf{RF}*}\mathbf{H}_{\mathbf{SI},n}\mathbf{F}_{\mathbf{BS}}^{\mathbf{RF}}\mathbf{F}_{\mathbf{BS},n}^{\mathbf{BB}}, \tag{14}$$

- The SI level at the ℓ-th RX RF chain at the BS is

$$\mathbf{c}_{\mathbf{SI},\ell,n} = \mathbf{w}_{\mathbf{BS},\ell}^{\mathbf{RF}*}\mathbf{H}_{\mathbf{SI},n}^{(\ell,:)}\mathbf{F}_{\mathbf{BS}}^{\mathbf{RF}}\mathbf{F}_{\mathbf{BS},n}^{\mathbf{BB}}, \tag{15}$$

- Suppress wideband SI at ℓ-th RX RF chain at BS

$$\mathbf{w}_{\mathbf{BS},\ell}^{\mathbf{RF}*}\underbrace{\left[\mathbf{H}_{\mathbf{SI},n_1}^{(\ell,:)}\mathbf{F}_{\mathbf{BS}}^{\mathbf{RF}}\mathbf{F}_{\mathbf{BS},n_1}^{\mathbf{BB}},\ldots,\mathbf{H}_{\mathbf{SI},n_{\mathcal{N}_{\mathbf{freq}}}}^{(\ell,:)}\mathbf{F}_{\mathbf{BS}}^{\mathbf{RF}}\mathbf{F}_{\mathbf{BS},n_{\mathcal{N}_{\mathbf{freq}}}}^{\mathbf{BB}}\right]}_{\mathbf{B}_\ell} = 0^T \tag{16}$$

- Goal: minimize the gain of the SI channel at the ℓ-th RX RF chain

$$\begin{aligned}&\min_{\mathbf{w}_{\mathbf{BS},\ell}^{\mathbf{RF}}} \|\mathbf{w}_{\mathbf{BS},\ell}^{\mathbf{RF}}\mathbf{B}_\ell\|_F^2\\ &\text{s.t. } \mathbf{w}_{\mathbf{BS},\ell}^{\mathbf{RF}} \in \mathbb{V}_{b_r}^{\left(N_{\mathbf{BS}}^{\mathbf{RX}}/L_{\mathbf{RX}}\right)\times 1},\ \ell = 1,\ldots,L_{\mathbf{RX}}\end{aligned} \tag{17}$$

Baseband Beamforming

- Goal: maximize the beamformed power and suppress the residual SI and MUI

$$\mathbf{w}_{\mathrm{BS},u,n}^{\mathrm{BB}*} \underbrace{\left[\underbrace{\mathbf{W}_{\mathrm{BS}}^{\mathrm{RF}*}\mathbf{H}_{\mathrm{SI},n}\mathbf{F}_{\mathrm{BS}}^{\mathrm{RF}}\mathbf{F}_{\mathrm{BS},n}^{\mathrm{BB}}}_{K \text{ Residual SI Nulls}}, \underbrace{\left[\mathbf{W}_{\mathrm{BS}}^{\mathrm{RF}*}\mathbf{H}_{u,n}\mathbf{f}_{u,n}\right]_{\substack{u=0 \\ u\neq u}}^{U-1}}_{U-1 \text{ MUI Nulls}} \right]}_{\mathbf{D}_{u,n}} = \mathbf{w}_{\mathrm{BS},u,n}^{\mathrm{BB}*}\mathbf{D}_{u,n} = 0^{T}, \tag{18}$$

- Subsequently, the optimization problem of the baseband combiner is

$$\begin{aligned} &\max_{\mathbf{w}_{\mathrm{BS},u,n}^{\mathrm{BB}}} \; |\mathbf{w}_{\mathrm{BS},u,n}^{\mathrm{BB}*}\mathbf{W}_{\mathrm{BS}}^{\mathrm{RF}*}\mathbf{H}_{u,n}\mathbf{f}_{u,n}|^{2} \\ &\text{s.t. } \|\mathbf{W}_{\mathrm{BS}}^{\mathrm{RF}}\mathbf{w}_{\mathrm{BS},u,n}^{\mathrm{BB}}\| = 1, \forall u, \\ &\mathbf{w}_{\mathrm{BS},u,n}^{\mathrm{BB}*}\mathbf{D}_{u,n} = 0^{T}, \; \forall u. \end{aligned} \tag{19}$$

- Then the solution is given in two-steps
  1. Matched filter $\tilde{\mathbf{w}}_{\mathrm{BS},u,n}^{\mathrm{BB}} = \mathbf{W}_{\mathrm{BS}}^{\mathrm{RF}*}\mathbf{H}_{u,n}\mathbf{f}_{u,n}$ (Maximize beamformed power)
  2. $\mathbf{w}_{\mathrm{BS},u,n}^{\mathrm{BB}} = \underbrace{(\mathbf{I} - \mathbf{D}_{u,n}\mathbf{D}_{u,n}^{\dagger})}_{\text{Interference Null-Space}} \tilde{\mathbf{w}}_{\mathrm{BS},u,n}^{\mathrm{BB}}$ (Suppress interference)
  3. Beamformers are coupled, then, iterative routine until convergence

Numerical Results

Table 3: Simulation Parameters (Wideband)

Parameter	Value
Carrier frequency	28 GHz
Bandwidth	500 MHz
Subcarrier spacing	120 kHz
Number of active subcarriers	3749
Number of antennas at BS sub-array	32
Number of antennas at user	8
Number of TX/RX RF chains	4
Number of uplink/downlink users	2
Phase shifter quantization bits	4
Downlink TX power	10 W
Power of RF chain	100 mW
Power of phase shifter	10 mW
Power amplifier	100 mW

Xianghao Yu, Juei-Chin Shen, Jun Zhang, and Khaled B. Letaief. Alternating Minimization Algorithms for Hybrid Precoding in Millimeter Wave MIMO Systems. In: *IEEE Journal of Selected Topics in Signal Processing* 10.3 (2016), pp. 485–500.

Carlos Baquero Barneto, Taneli Riihonen, Sahan Damith Liyanaarachchi, Mikko Heino, Nuria González-Prelcic, and Mikko Valkama. Beamformer Design and Optimization for Joint Communication and Full-Duplex Sensing at mm-Waves. In: *IEEE Transactions on Communications* 70.12 (2022), pp. 8298–8312.

Beam-Pattern

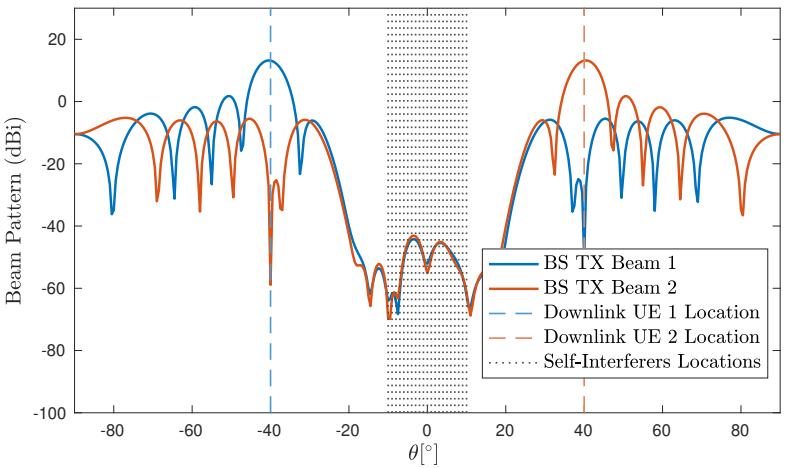

(a) Line-of-Sight Self-Interference

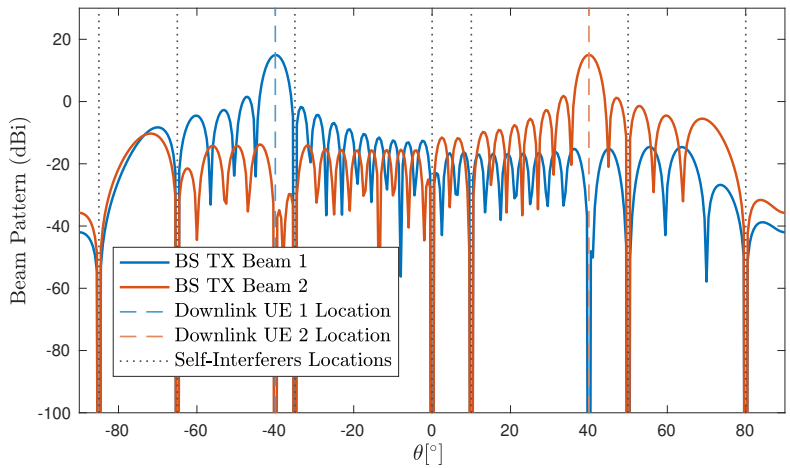

(b) Non-Line-of-Sight Self-Interference

Optimized effective TX Beampattern of BS

- Joint beamforming design simultaneously allows for
  1. Maximizing beamformed power towards intended users
  2. Suppressing multiuser interference and self-interference

Self-Interference

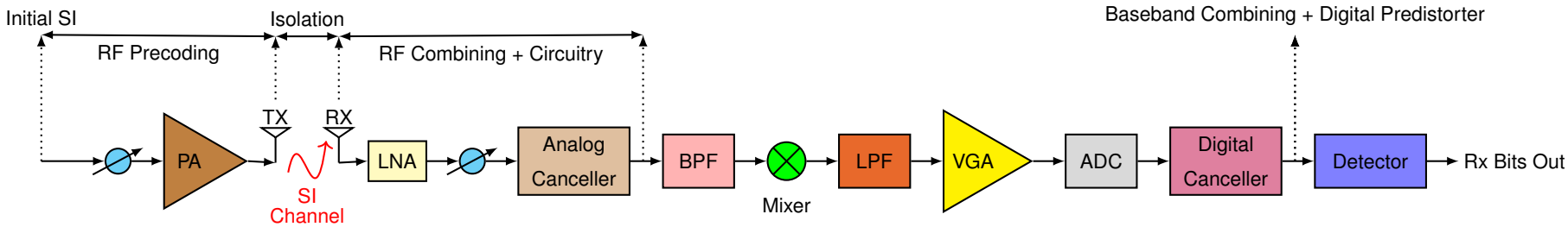

Tracking the interference levels across the entire BS transceiver blocks

- Multi-stage self-interference suppression:
  1. From Initial to LNA: 80 dB reduction
     (50 dB) from RF precoding (F_{BS}^{RF})
     (30 dB) from RF isolation
  2. From LNA to ADC input: 70 dB reduction
     (50 dB) from RF combining (W_{BS}^{RF})
     (20 dB) from analog circuitry
  3. Digital circuitry & beamforming: SI level maintained at -300 dB

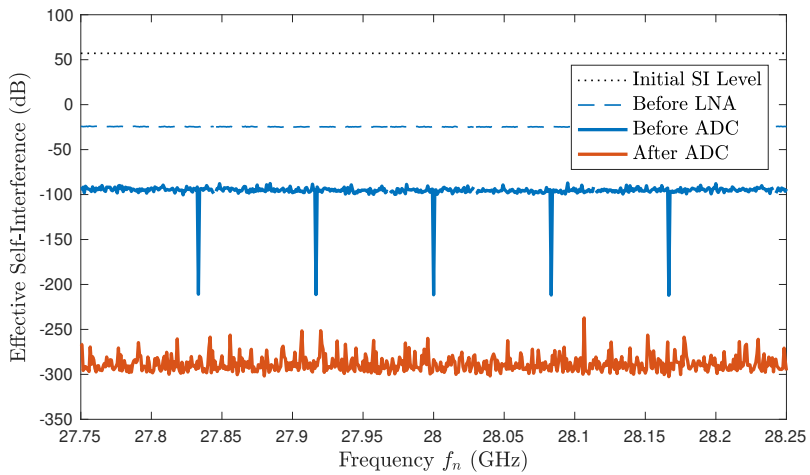

Self-interference suppression at multiple stages

PA: power amplifier, LNA: low noise amplifier, BPF: bandpass filter, LPF: lowpass filter, VGA: variable gain amplifier, ADC: analog-to-digital converter

Self-Interference

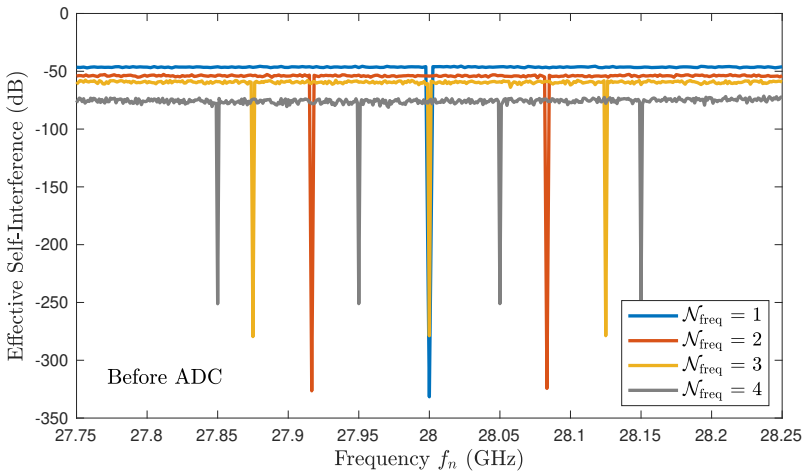

(a)

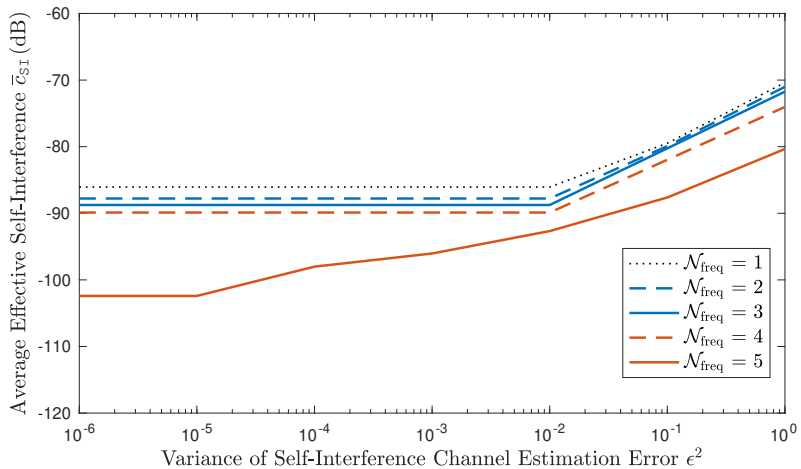

(b)

(a) Effect of the number of nulling subcarriers. (b) Effect of the self-interference channel estimation error

- Increasing the number of nulling subcarriers:
  1. Analog beamformers become robust against SI
  2. Average SI decreases
- Average SI increases with the channel estimation error (additional source of interference)

Spectral Efficiency

- Previous approaches saturated by interference, since unit modulus violates the interference suppression constraint
- Minor gap with “RM", analog precoder $\mathbf{F}_{\mathrm{BS}}^{\mathrm{RF}}$ solely designed to maximize the beamformed vs. our approach (maximize beamformed power + suppress SI)
- Gap with all-digital: reduction in RF chains + unit modulus constraint (steering the beams using only the phase shifters; phased arrays)

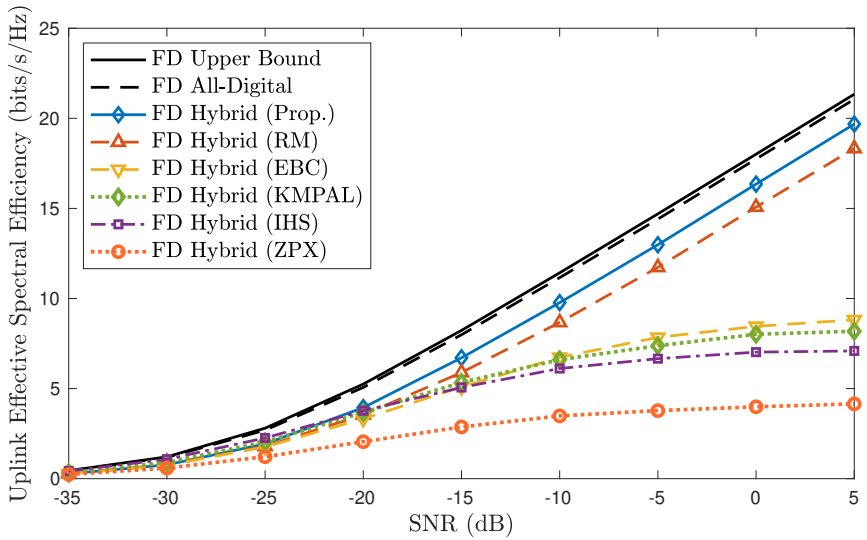

Roberto López-Valcarce and Marcos Martínez-Cotelo. Full-Duplex mmWave MIMO With Finite-Resolution Phase Shifters. In: *IEEE Transactions on Wireless Communications* 21.11 (2022), pp. 8979–8994.

Elyes Balti, Chris Dick, and Brian L. Evans. Low Complexity Hybrid Beamforming for mmWave Full-Duplex Integrated Access and Backhaul. In: *IEEE Global Comm. Conf.* 2022, pp. 1606–1611.

K. Satyanarayana, Mohammed El-Hajjar, Ping-Heng Kuo, Alain Mourad, and Lajos Hanzo. Hybrid Beamforming Design for Full-Duplex Millimeter Wave Communication. In: *IEEE Transactions on Vehicular Technology* 68.2 (2019), pp. 1394–1404.

Ian P. Roberts, Hardik B. Jain, and Sriram Vishwanath. Frequency-Selective Beamforming Cancellation Design for Millimeter-Wave Full-Duplex. In: *IEEE International Conference on Communications (ICC)*. 2020, pp. 1–6.

Zhenyu Xiao, Pengfei Xia, and Xiang-Gen Xia. Full-Duplex Millimeter-Wave Communication. In: *IEEE Wireless Communications* 24.6 (2017), pp. 136–143.

Energy Efficiency: Architectures & # RF Chains

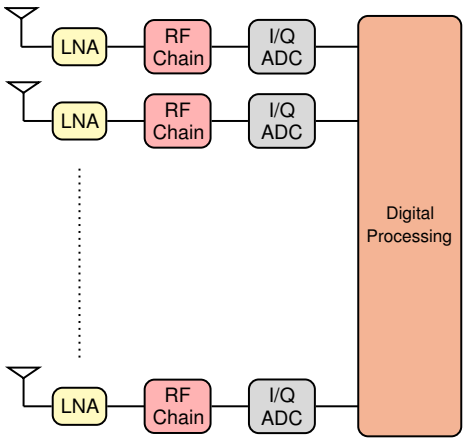

(a) All-Digital

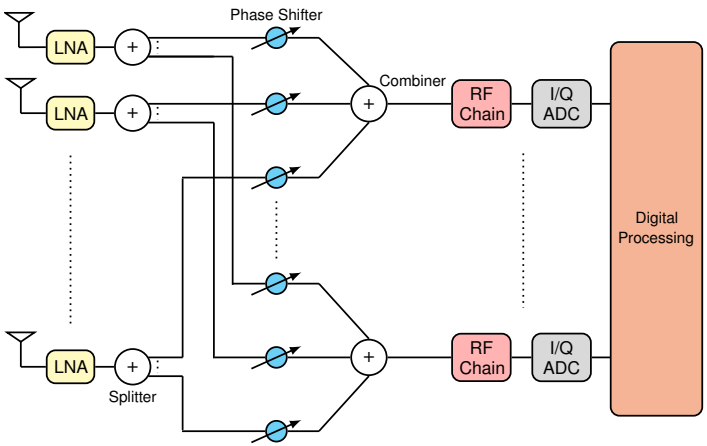

(b) Hybrid Fully-Connected

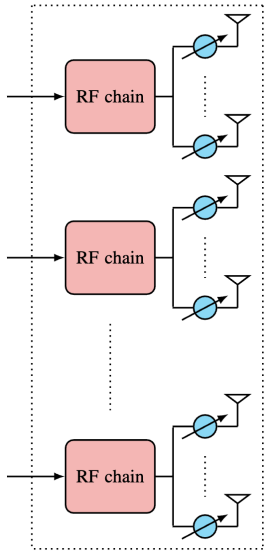

(c) Hybrid Partially-Connected

- Energy efficiency $= \frac{\text{Spectral efficiency}}{\text{Power consumption}}$
- All-digital consumes hefty power
- Hybrid has reduced # RF chains
- Partially-connected is the best energy-efficient architecture

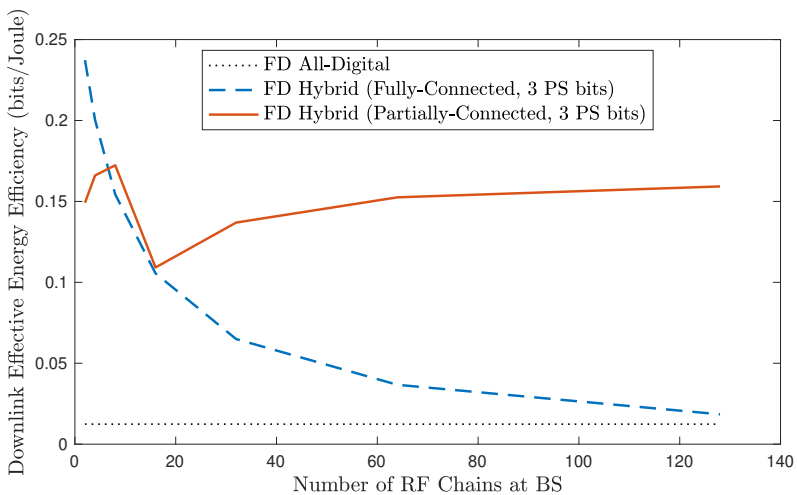

Outline

Conclusion

- **Motivation**: Providing low-latency, high data-rate cellular communications using full duplex
- **Problem**: LNAs and ADCs saturated by interference
- **Approach**: Use degrees of freedom to suppress interference and achieve high data rate
- **Proposed Solution**: Joint analog-digital beamforming design
  1. Reduce large amount of interference in the analog domain to avoid the LNAs and ADCs saturation
  2. Allocate degrees of freedom between interference cancellation and spatial multiplexing gain in a balanced way
- **Takeaways**: The proposed joint analog-digital beamforming design
  1. increasing # BS antennas from 4 to 128: reduces the interference by 120 dB and double the data rates from 6.7 to 14 bits/s/Hz
  2. Fast convergence in 3-5 iterations: Achieves 180 dB reduction in interference in analog domain and 25 dB increase in uplink SINR
  3. Increasing # of nulling subcarriers increases robustness of analog beamformers against SI
  4. Increasing SNR increases the gain in data rate of full duplex vs. half duplex systems

Outline

Conference Papers: Full-Duplex Communications

1. **E. Balti**, C. Dick, and B. L. Evans, “Low Complexity Hybrid Beamforming for mmWave Full-Duplex Integrated Access and Backhaul," in *IEEE Global Communications Conference (Globecom)*, Brazil, 2022
2. **E. Balti**, and B. L. Evans, “Full-Duplex Massive MIMO Cellular Networks with Low Resolution ADC/DAC," in *IEEE Global Communications Conference (Globecom)*, Brazil, 2022
3. **E. Balti**, and B. L. Evans, “Reverse Link Analysis for Full-Duplex Cellular Networks with Low Resolution ADC/DAC," in *IEEE Signal Processing Advances in Wireless Communications*, Finland, 2022
4. **E. Balti**, and B. L. Evans, “Forward Link Analysis for Full-Duplex Cellular Networks with Low Resolution ADC/DAC," in *IEEE Signal Processing Advances in Wireles Communications*, Finland, 2022
5. **E. Balti**, and N. Mensi, “Zero-Forcing Max-Power Beamforming for Hybrid mmWave Full-Duplex MIMO Systems," in *IEEE International Conference on Advanced Systems and Emergent Technologies*, Tunisia, 2020

Journal Papers: Full-Duplex Communications

1. **E. Balti**, and B. L. Evans, “A Unified Framework for Full-Duplex Massive MIMO Cellular Networks with Low Resolution Data Converters,” in *IEEE Open Journal of the Communications Society*, vol. 4, pp. 1-28, 2023
2. **E. Balti**, S. Akoum, I. Alfalujah, and B. L. Evans, “Hybrid Beamforming Design For Full-Duplex Millimeter Wave Massive MIMO Systems,” in *IEEE Trans. Veh. Technol.*, vol. 73, pp. 17041-17058, 2024
3. **E. Balti**, and B. L. Evans, “Millimeter Wave Full-Duplex Massive MIMO: Beamforming and System Design Tradeoffs,” *submitted to IEEE Trans. Wireless Commun.* [**under review**]
4. **E. Balti**, K. Tinsley, and B. L. Evans, “Millimeter Wave Full-Duplex Multiuser MIMO: Joint Beamforming Design and Optimization,” *submitted to IEEE Journal on Selected Areas in Commun.* [**under review**]
5. **E. Balti**, S. Akoum, I. Alfalujah, and B. L. Evans, “Hybrid Beamforming Design for Wideband mmWave Full-Duplex Systems," *submitted to IEEE Trans. Green Commun. Netw.*", [**under review**]
6. **E. Balti**, S. Akoum, I. Alfalujah, M. Majmundar, C. Dick, K. Tinsley, and B. L. Evans, “An Overview of Signal Processing Techniques for Full-Duplex Systems,” [**in preparation**]
7. **E. Balti**, S. Akoum, I. Alfalujah, M. Majmundar, C. Dick, K. Tinsley, and B. L. Evans, “Millimeter Wave Full-Duplex Radios: Application on Joint Communication and Sensing,” [**in preparation**]

Conference Papers: RIS, Vehicular Networks & Relays

1. P. Nuti, **E. Balti**, and B. L. Evans,“Spectral Efficiency Optimization for mmWave Wideband MIMO RIS-assisted Communication,” in *IEEE VTC*, Finland, 2022
2. N. Mensi, D. B. Rawat, and **E. Balti**, “Physical Layer Security for V2I Communications: Reflecting Surfaces vs. Relaying," in *IEEE GLOBECOM*, Spain, 2021
3. N. Mensi, D. B. Rawat, and **E. Balti**, “PLS for V2I Communications Using Friendly Jammer and Double kappa-mu Shadowed Fading," in *IEEE ICC*, Canada, 2021
4. **E. Balti**, M. Guizani, B. Hamdaoui, and B. Khalfi, “Mixed RF/FSO Relaying Systems with Hardware Impairments," in *IEEE GLOBECOM*, Singapore, 2017
5. **E. Balti**, M. Guizani, and B. Hamdaoui, “Hybrid Rayleigh and Double-Weibull over impaired RF/FSO system with outdated CSI," in *IEEE ICC*, France, 2017
6. **E. Balti**, M. Guizani, B. Hamdaoui, and Y. Maalej, “Partial Relay Selection for Hybrid RF/FSO Systems with Hardware Impairments," in *IEEE GLOBECOM*, Washington D.C., 2016
7. Y. Maalej, A. Abderrahim, M. Guizani, B. Hamdaoui, and **E. Balti**, “Advanced Activity-Aware Multi-Channel Operations 1609.4 in VANETs for Vehicular Clouds," in *IEEE GLOBECOM*, Washington D.C., 2016

Journal Papers: Backhaul, Relays & Smart Grid Comm.

1. N. Mensi, D. B. Rawat, and **E. Balti**, “Gradient Ascent Algorithm for Enhancing Secrecy Rate in Wireless Communications for Smart Grid," *IEEE Trans. Green Commun. and Networking,* vol. 6, no. 1, pp. 107-116, Mar. 2022
2. **E. Balti**, and B. K. Johnson, “On The Joint Effects of HPA Nonlinearities and IQ Imbalance On Mixed RF/FSO Cooperative Systems,” *IEEE Trans. Commun.,* vol. 69, no. 11, pp. 7879-7894, Nov. 2021
3. **E. Balti**, and B. K. Johnson, “Tractable Approach to MmWaves Cellular Analysis with FSO Backhauling under Feedback Delay and Hardware Limitations," *IEEE Trans. Wireless Commun.,* vol. 19, no. 1, pp. 410-422, Jan. 2020
4. **E. Balti**, and M. Guizani, “Mixed RF/FSO Cooperative Relaying Systems with Co-Channel Interference," *IEEE Trans. Commun.,* vol. 66, no. 9, pp. 4014-4027, Sept. 2018
5. **E. Balti**, M. Guizani, B. Hamdaoui, and B. Khalfi, "Aggregate Hardware Impairments Over Mixed RF/FSO Relaying Systems With Outdated CSI," *IEEE Trans. Commun.*, vol. 66, no. 3, pp. 1110-1123, Mar. 2018
6. **E. Balti**, and M. Guizani, “Impact of Non-Linear High-Power Amplifiers on Cooperative Relaying Systems," *IEEE Trans. Commun.*, vol. 65, no. 10, pp. 4163-4175, Oct. 2017

Thanks for you attention
Questions ?

Back-Up

Future Research Directions

Direction #1: Reconfigurable Intelligent Surfaces (RISs)

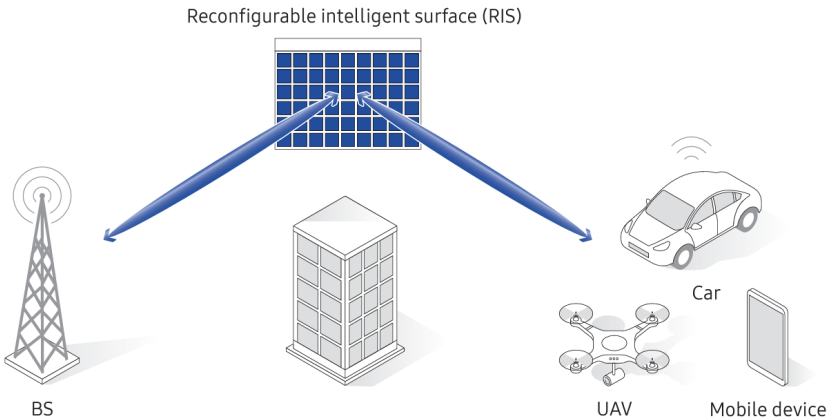

(a) RIS-aided communication when the line-of-sight path is blocked

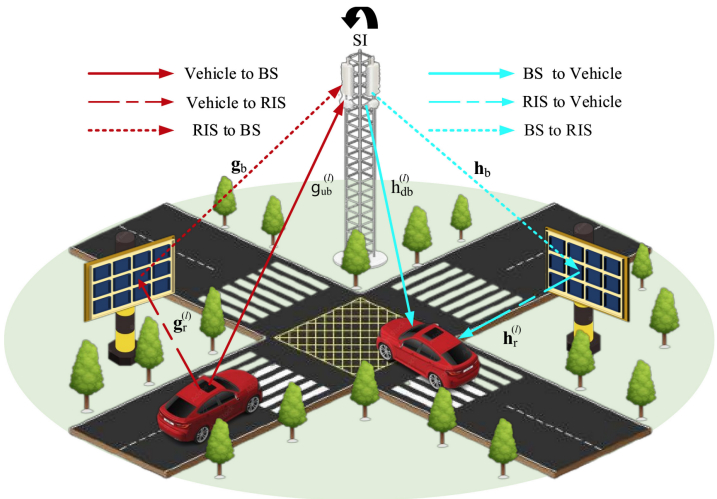

(b) RIS-assisted full-duplex systems

- (Left) RIS provides an alternative path when the line-of-sight path is blocked
- (Right) Deployed in a various uses cases such as V2X and unmanned aerial vehicles to extend the coverage and improve the network scalability
- (Right) Assists in self-interference mitigation
- (Right) RIS-assisted calibration of base stations (of interest to test & measurement companies)

Direction #2: Integrated Sensing and Communication

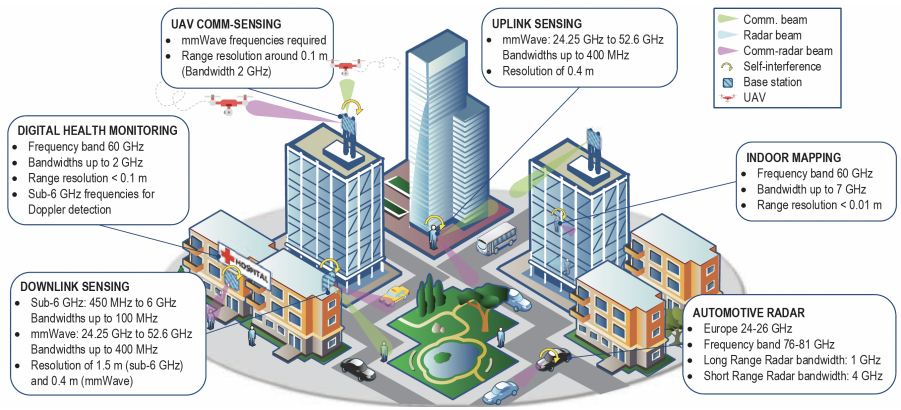

(a) Integrated sensing and communication

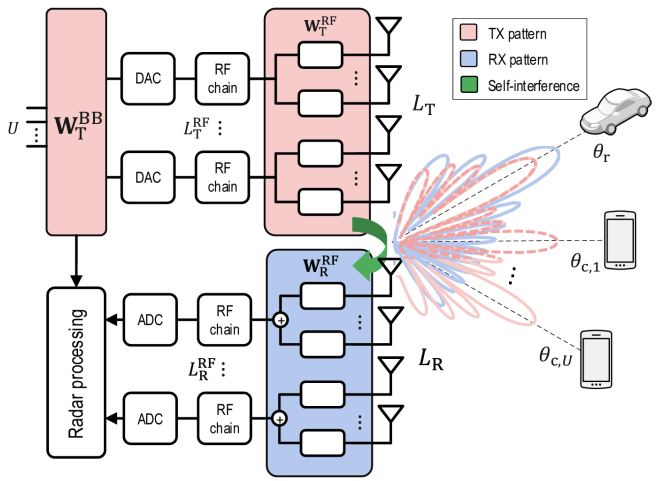

(b) With full-duplex hybrid beamforming

- Leveraging AI and ML to enhance the performance of ISAC systems, including adaptive beamforming, object detection, and predictive analytics
- Optimizing the use of the radio frequency spectrum to ensure that sensing and communication tasks do not interfere with each other
- Designing waveforms and signal processing techniques optimized for full-duplex operation to support high-quality communication and high-resolution sensing

Direction #3: 5G/6G Enhanced ADAS (V2X)

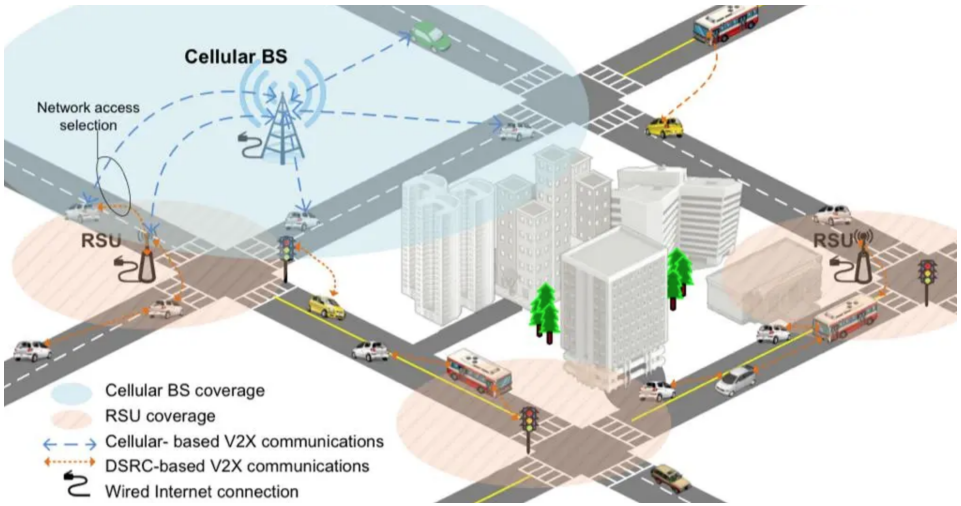

V2X communications in a hybrid dedicated short range communication (DSRC) and cellular architecture

- Integration of machine learning for predictive modeling and intelligent-decision making, thus enhance Advanced Driving Awareness Systems (ADAS)
- Incorporate sensing and address interference between autonomous vehicles
- Develop necessary theory, experiments and algorithms:
    1. High data rate collaborative sensing among multiple vehicles
    2. Robust and secure vehicle automation
    3. Development of situational 5G/6G data rate map
    4. Multi-antenna strategies for mmWave vehicular-to-infrastructure communication aided by sub-7 GHz systems

Background

Cross-Division Duplexing (XDD)

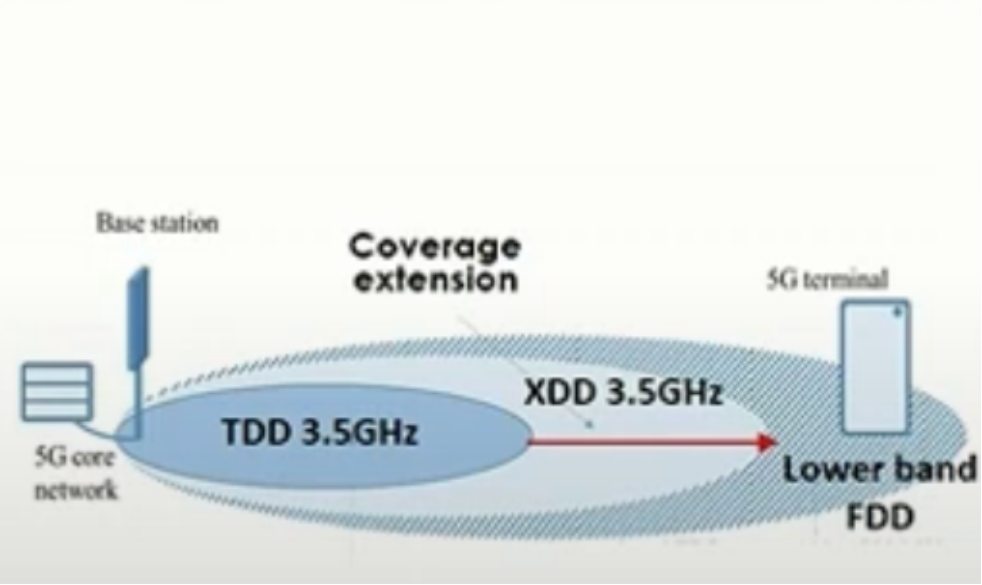

TDD Coverage Extension through XDD

Self-Interference Channel: Rician Model

- The aggregate SI channel is

$$\mathbf{H}_{\mathrm{SI}} = \underbrace{\sqrt{\frac{\kappa}{\kappa+1}}\mathbf{H}_{\mathrm{LOS}}}_{\text{Near-Field}} + \underbrace{\sqrt{\frac{1}{\kappa+1}}\mathbf{H}_{\mathrm{NLOS}}}_{\text{Far-Field}} \quad (20)$$

- The (q, p)-th entry of the LOS SI leakage matrix can be written as

$$[\mathbf{H}_{\mathrm{LOS}}]_{qp} = \frac{1}{r_{pq}} e^{-i2\pi \frac{r_{pq}}{\lambda}} \quad (21)$$

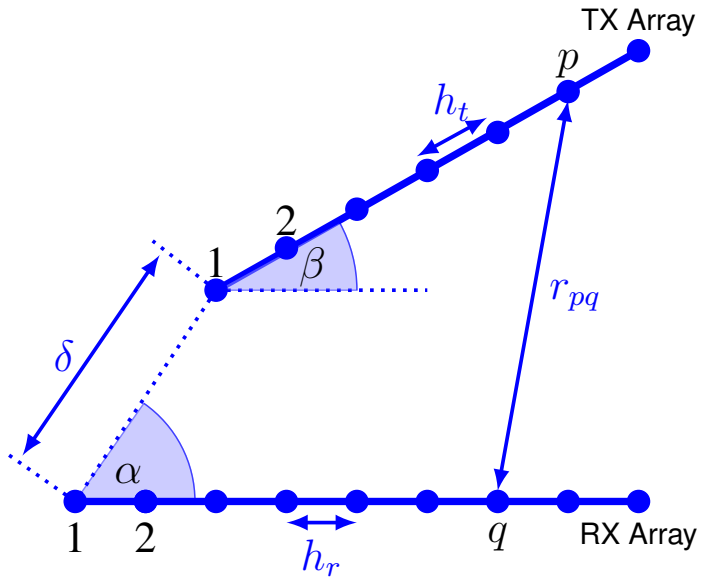

Full-Duplex Transceiver Arrays

$$r_{pq} = \sqrt{(\delta\cos\beta + (p-1)h_t\cos\alpha - (q-1)h_r)^2 + (\delta\sin\beta + (p-1)h_t\sin\alpha)^2} \quad (22)$$

Self-Interference Channel: Empirical AT&T Model

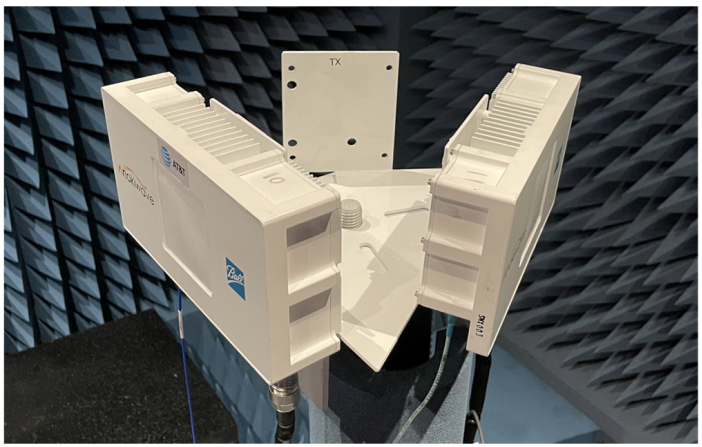

(a)

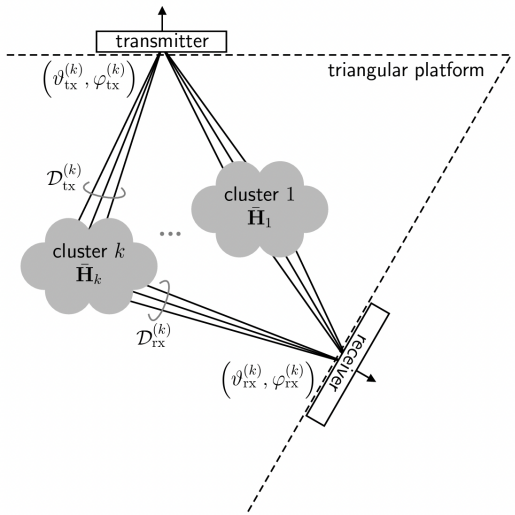

(b)

(a) 28 GHz Phased array measurement platform inside an anechoic chamber; receive array on left and transmit array on right. (b) Coupling clusters comprising the coarse geometric model of the self-interference channel

The channel matrix produced by the k-th cluster is given by

$$\mathsf{H}_k = \sum_{(\theta_{\mathbf{tx}},\phi_{\mathbf{tx}})\in\mathcal{D}_{\mathbf{tx}}^{(k)}} \sum_{(\theta_{\mathbf{rx}},\phi_{\mathbf{rx}})\in\mathcal{D}_{\mathbf{rx}}} \mathsf{a}_{\text{rx}}(\theta_{\text{rx}},\phi_{\text{rx}})\mathsf{a}_{\text{tx}}(\theta_{\text{tx}},\phi_{\text{tx}})^*$$

The resulting channel matrix comprising all the $\mathcal{N}_{\mathbf{clust}}$ is $\mathsf{H} = \sum_{k=1}^{\mathcal{N}_{\mathbf{clust}}} \mathsf{H}_k \frac{\sqrt{N_{\text{rx}} N_{\text{tx}}}}{\| \sum_{k=1}^{\mathcal{N}_{\mathbf{clust}}} \mathsf{H}_k \|_F}$

Ian P. Roberts, Aditya Chopra, Thomas Novlan, Sriram Vishwanath, and Jeffrey G. Andrews. Spatial and Statistical Modeling of Multi-Panel Millimeter Wave Self-Interference. In: *IEEE Journal on Selected Areas in Communications* 41.9 (2023), pp. 2780–2795.

What is Beamforming ?

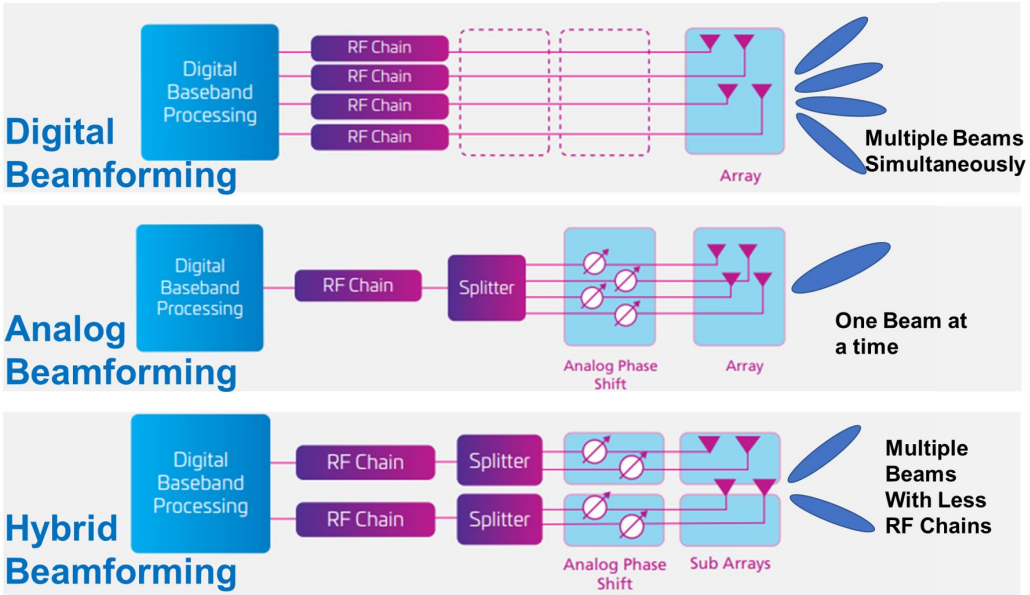

1. **Digital Beamforming**: *All signal processing in digital baseband*
   - Each antenna has its own dedicated RF chain
   - Simultaneously synthesizes multiple beams to serve multiple users
2. **Analog Beamforming**: *All signal processing in analog*
   - Has single RF chain and serves only one user at a time
3. **Hybrid Beamforming**: *Signal processing split between analog and digital*
   - Reduced number of RF chains, fewer than number of antennas
   - Serves multiple users

Contribution 1: Point-to-Point Systems

System Model

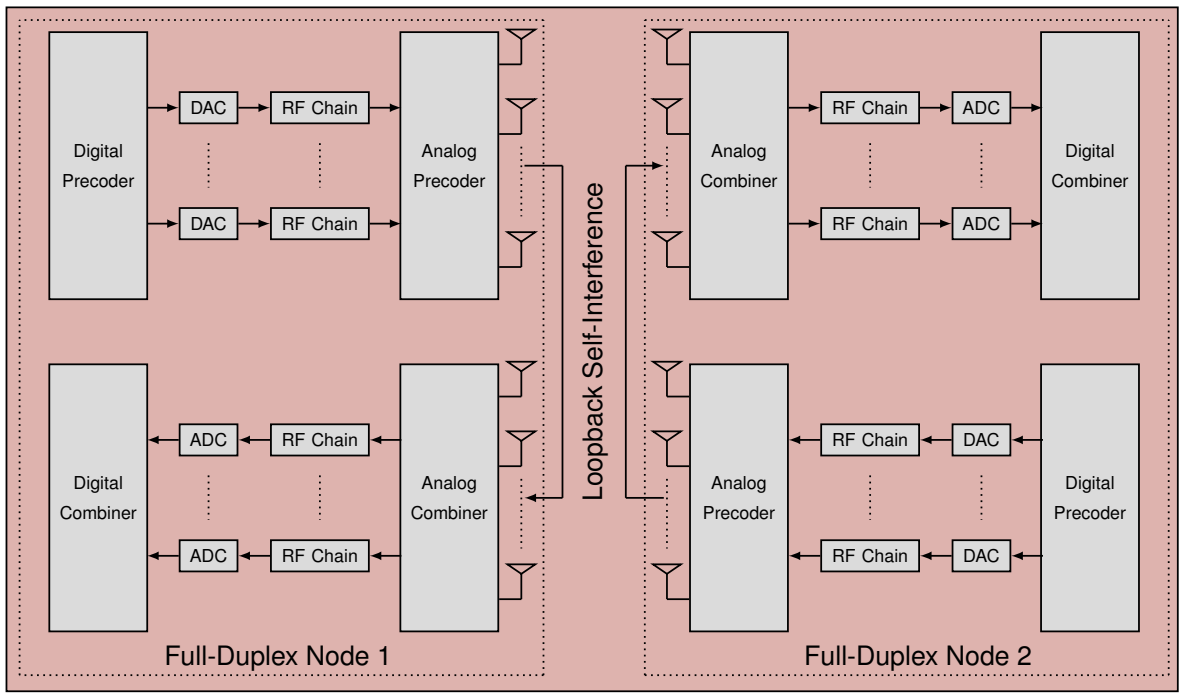

Hybrid analog/digital architecture of a point-to-point two-node FD system

- The received signal at node n transmitted from node $m \neq n$ is given by

$$y_n = \underbrace{W_n^{BB*} W_n^{RF*} H_{nm} F_m^{RF} F_m^{BB} x_m}_{\text{Desired Signal}} + \underbrace{W_n^{BB*} W_n^{RF*} H_{nn} F_n^{RF} F_n^{BB} x_n}_{\text{Self-Interference Signal}} + \underbrace{W_n^{BB*} W_n^{RF*} n_n}_{\text{Filtered Noise}} \quad (23)$$

Beamforming

- We aim at minimizing the interference power while preserving the signal dimension, i.e., preserve the rank of the effective channel
- For analog beamforming, we first relax the unit modulus constraint to preserve the convexity of the problem and then introduce this constraint separately after the convergence
- Solve for the analog beamformers solution using the Lagrange approach
- We define problem to design the analog combiner at node n

$$\begin{aligned} \mathscr{P}_1 : \min_{\mathbf{W}_n^{\mathbf{RF}}} \ & \mathrm{Tr}\left(\mathbf{W}_n^{\mathbf{RF}*}\mathbf{R}_n\mathbf{W}_n^{\mathbf{RF}}\right) \\ \text{s.t. } & \mathbf{W}_n^{\mathbf{RF}*}\mathbf{H}_{nm}\mathbf{F}_m^{\mathbf{RF}} = \alpha \mathbf{I}_{N_{\mathbf{RF}}} \\ & \mathbf{W}_n^{\mathbf{RF}} \in \mathcal{W}_{\mathbf{RF}} \end{aligned} \tag{24}$$

- where α is the power normalization factor and $\mathbf{R}_n$ is the covariance of the precoded SI and noise

$$\mathbf{R}_n = \mathrm{inr}_n \mathbf{H}_{nn}\mathbf{F}_n^{\mathbf{RF}}\mathbf{F}_n^{\mathbf{RF}*}\mathbf{H}_{nn}^* + \mathbf{I} \tag{25}$$

- inr_n is the average large-scale SI power

Beamforming

Theorem

The unconstrained analog beamformers are expressed by

$$\tilde{W}_n^{RF} = \alpha R_n^{-1} H_{nm} \tilde{F}_m^{RF} \left(H_{nm} \tilde{F}_m^{RF*} R_n^{-1} H_{nm} \tilde{F}_m^{RF} \right)^{-1} \tag{26}$$

$$\tilde{F}_n^{RF} = \beta S_n^{-1} H_{mn}^{*} \tilde{W}_m^{RF} \left(\tilde{W}_m^{RF*} H_{mn} S_n^{-1} H_{mn}^{*} \tilde{W}_m^{RF} \right)^{-1} \tag{27}$$

where $S_n = \text{inr}_n H_{nn}^{*} W_n^{RF} W_n^{RF*} H_{nn} + I$, $\alpha = 1/\sqrt{\text{Tr}\left(\tilde{W}_n^{RF*} \tilde{W}_n^{RF} \right)}$ *and* $\beta = 1/\sqrt{\text{Tr}\left(\tilde{F}_n^{RF*} \tilde{F}_n^{RF} \right)}$ *are the normalization power coefficients, respectively.*

Remark

The beamforming solutions entailed by Theorem 1 are coupled. Hence, an iterative routine is carried out until the convergence

Spectral Efficiency and Self-Interference

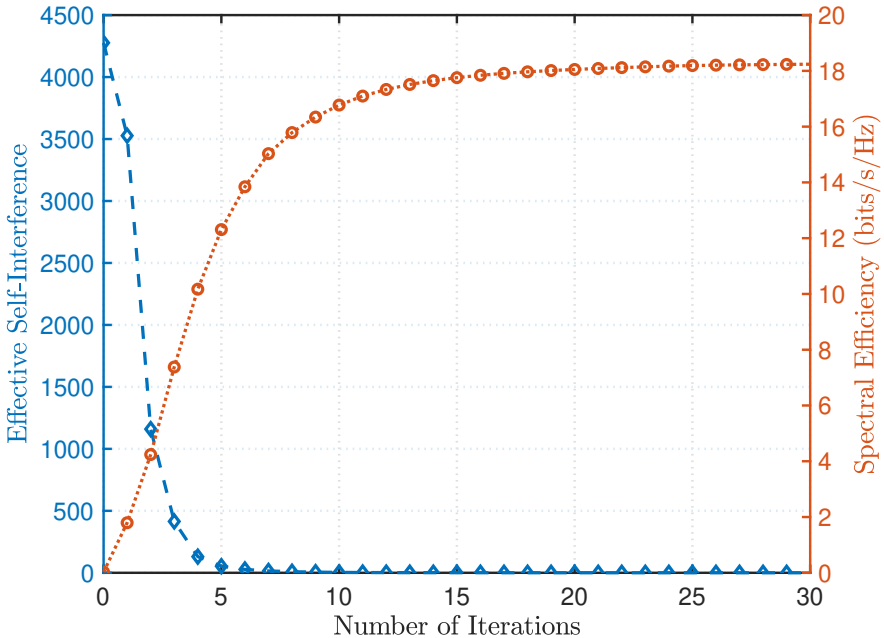

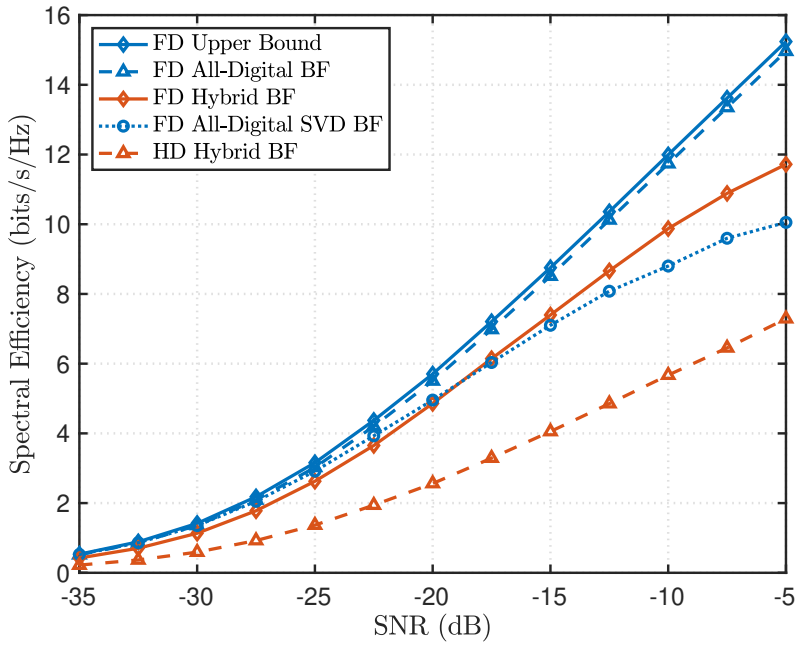

- (Left) Convergence in a few iterations (5-10)
- (left) Achieves about 45 dB reduction of SI in the analog domain
- (Left) Allocation of DoF between suppressing SI and increase spectral efficiency
- (Right) Outperform half-duplex (hybrid and all-digital)
- (Right) Gap with upperbound and all-digital due to the limited number of RF chains and unit-modulus constraint

Energy Efficiency # RF Chains, # Antennas

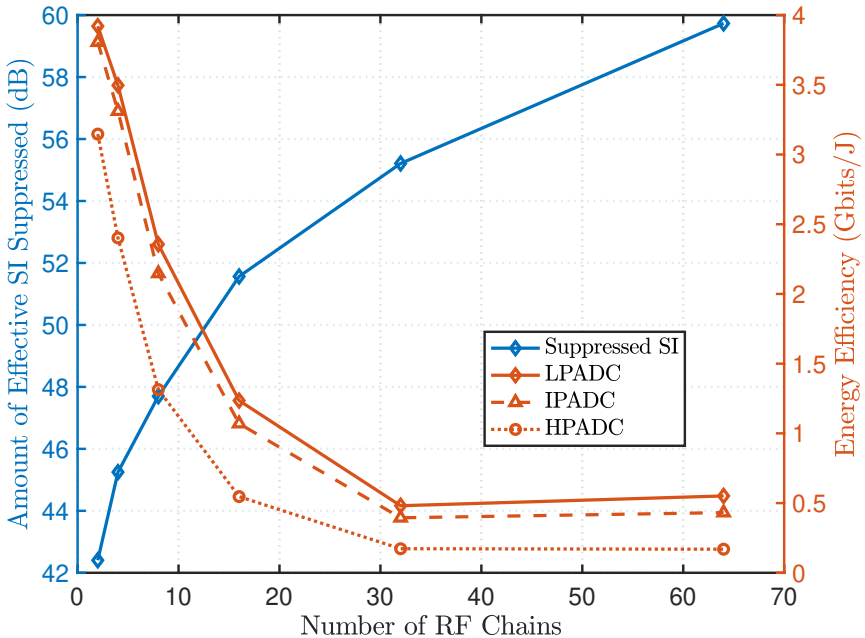

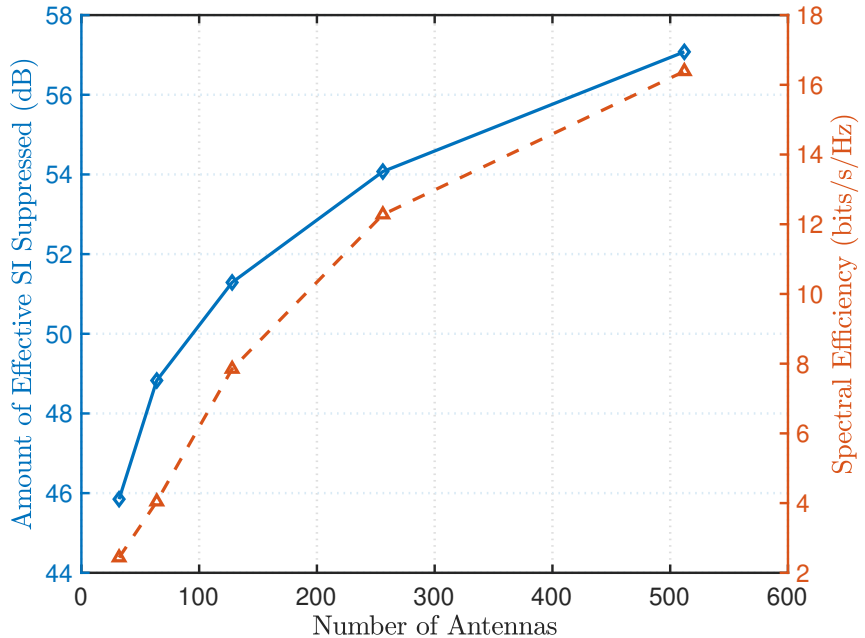

- (Left) Increasing # RF chains improves the SI suppression, but decreases the energy efficiency, since it consumes more power
- (Left) Low power ADCs achieve better energy efficiency
- (Right) increasing # antennas achieves higher SI reduction as well as enhancing the spectral efficiency

Phase shifter resolution

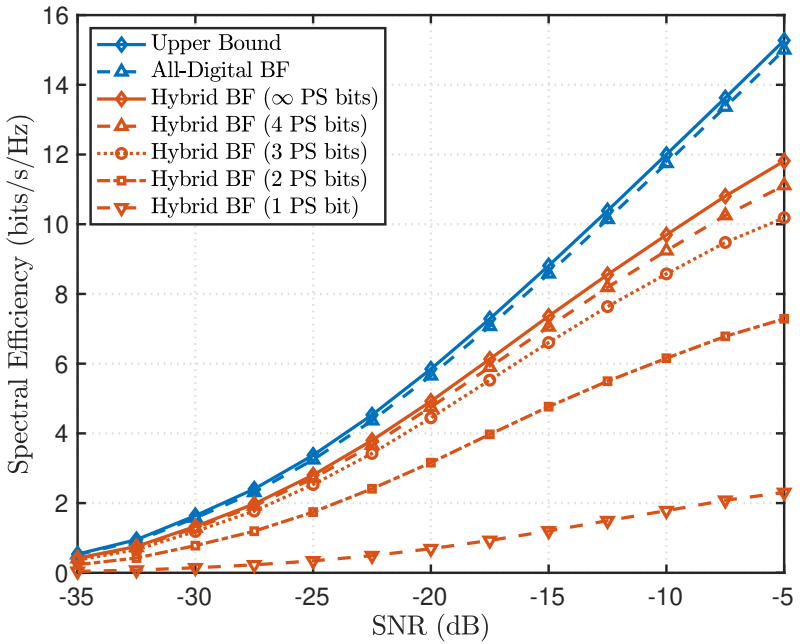

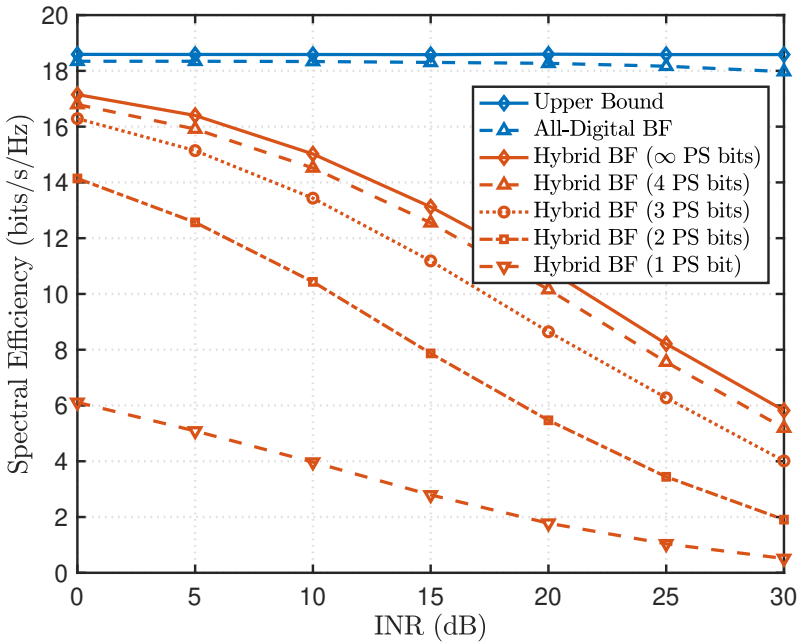

- ∞ phase shifter resolution achieves the best performance, however, it is not feasible
- 4 bits resolution are sufficient to achieve good performance
- lower resolution bits affect the beamforming accuracy, and then degrade performance

Contribution #1: Point-to-Point Full Duplex Hybrid Beamforming Systems

- **Problem**: Communication performance limited by loopback self-interference
- **Approach**: Use degrees of freedom to design hybrid analog-digital beamformers to cancel self-interference
- **Proposed Solution**: Joint analog-digital beamforming design:
  - Suppress large amount of interference in the analog domain to avoid the LNAs and ADCs saturation
  - Preserve the signal dimension (rank of the effective channel)
- **Takeaways**: The proposed solution achieves
  - Converge in a few iterations (5-10)
  - 45 dB reduction of SI in analog domain
  - 4 bits of phase shifter resolution are enough to achieve suffient SI reduction and better spectral efficiency

Contribution 2: Single-User MIMO

All-Digital Beamforming

- We aim at minimizing the interference power while preserving the signal dimension, i.e., preserve the rank of the effective channel
- We define the first subproblem to design the combiner at the BS as follows

$$\begin{aligned} \mathscr{P}_1 : \min_{\mathbf{W_{BS}}} \ & \mathrm{Tr}\left(\mathbf{W}_{\mathbf{BS}}^{\mathbf{RF}*}\mathbf{R}_1\mathbf{W}_{\mathbf{BS}}^{\mathbf{RF}}\right) \\ \text{s.t. } & \mathbf{W}_{\mathbf{BS}}^{*}\mathbf{H}_{\mathbf{u}}\mathbf{F}_{\mathbf{UE}} = \alpha \mathbf{I}_{N_{\mathbf{BS}}} \end{aligned} \tag{28}$$

- Where $\mathbf{R}_1$ is the covariance matrix of the precoded SI and noise at BS defined by

$$\mathbf{R}_1 = \rho_{\mathbf{s}}\mathbf{H}_{\mathbf{s}}\mathbf{F}_{\mathbf{BS}}\mathbf{F}_{\mathbf{BS}}^{*}\mathbf{H}_{\mathbf{s}}^{*} + \sigma^2\mathbf{I}_{N_{\mathbf{BS}}} \tag{29}$$

- Note that $\mathbf{R}_1$ is a positive definite matrix ($\mathbf{R}_1 > 0$) and $\alpha = 1/\sqrt{\mathrm{Tr}\left(\mathbf{W}_{\mathbf{BS}}^{*}\mathbf{W}_{\mathbf{BS}}\right)}$ is a power normalization coefficient

All-Digital Beamforming

- Similarly, we define the last three subproblems to design the beamformers as

$$\mathscr{P}_2 : \min_{\mathbf{F_{BS}}} \mathrm{Tr}\left(F_{BS}^* R_2 F_{BS}\right) \quad \text{s.t. } W_{UE}^* H_d F_{BS} = \beta I_{N_{BS}} \tag{30}$$

$$\mathscr{P}_3 : \min_{\mathbf{W_{UE}}} \mathrm{Tr}\left(W_{UE}^* R_3 W_{UE}\right) \quad \text{s.t. } W_{UE}^* H_d F_{BS} = \gamma I_{N_{BS}} \tag{31}$$

$$\mathscr{P}_4 : \min_{\mathbf{F_{UE}}} \mathrm{Tr}\left(F_{UE}^* R_4 F_{UE}\right) \quad \text{s.t. } W_{BS}^* H_u F_{UE} = \zeta I_{N_{BS}} \tag{32}$$

where R_2, R_3 and R_4 are given by

$$R_2 = \rho_s H_s^* W_{BS} W_{BS}^* H_s + \sigma_{BS}^2 I_{N_{BS}} \tag{33}$$

$$R_3 = \rho_{iui} H_{iui} F_{UE} F_{UE}^* H_{iui}^* + \sigma_{UE}^2 I_{N_{UE}} \tag{34}$$

$$R_4 = \rho_{iui} H_{iui}^* W_{UE} W_{UE}^* H_{iui} + \sigma_{UE}^2 I_{N_{UE}} \tag{35}$$

All-Digital Beamforming

Theorem

The optimal combiners and precoders at the BS and UEs, solutions to the problems (28,30,31 and 32) are expressed by

$$W_{BS} = \alpha R_1^{-1} H_u F_{UE} \left(F_{UE}^* H_u^* R_1^{-1} H_u F_{UE} \right)^{-1} \tag{36}$$

$$F_{BS} = \beta R_2^{-1} H_d^* W_{UE}^* \left(W_{UE}^* H_d R_2^{-1} H_d^* W_{UE} \right)^{-1} \tag{37}$$

$$W_{UE} = \gamma R_3^{-1} H_d F_{BS} \left(F_{BS}^* H_d^* R_3^{-1} H_d F_{BS} \right)^{-1} \tag{38}$$

$$F_{UE} = \zeta R_4^{-1} H_u^* W_{BS}^* \left(W_{BS}^* H_u R_4^{-1} H_u^* W_{BS} \right)^{-1} \tag{39}$$

Remark

The beamforming solutions entailed by Theorem 2 are coupled. Hence, an iterative routine is carried out until the convergence

Convergence

- The effective interference powers (objective functions) are given by

$$\mathcal{J}_1 = \mathrm{Tr}\left(\rho_s W_{BS}^* H_s F_{BS} F_{BS}^* H_s^* W_{BS}\right) \tag{40}$$

$$\mathcal{J}_2 = \mathrm{Tr}\left(\rho_s F_{BS}^* H_s^* W_{BS} W_{BS}^* H_s F_{BS}\right) \tag{41}$$

$$\mathcal{J}_3 = \mathrm{Tr}\left(\rho_{iui} W_{UE}^* H_{iui} F_{UE} F_{UE}^* H_{iui}^* W_{UE}\right) \tag{42}$$

$$\mathcal{J}_4 = \mathrm{Tr}\left(\rho_{iui} F_{UE}^* H_{iui}^* W_{UE} W_{UE}^* H_{iui} F_{UE}\right) \tag{43}$$

Table 4: Comparative Analysis of Beamforming Normalization Techniques

Metrics	Every Iteration	After Convergence
Performance (Effective SI)	✓	✗
Computational Cost	✗	✓
Rate of Convergence	✗	✓
Convergence Stability	✓	✗

Convergence

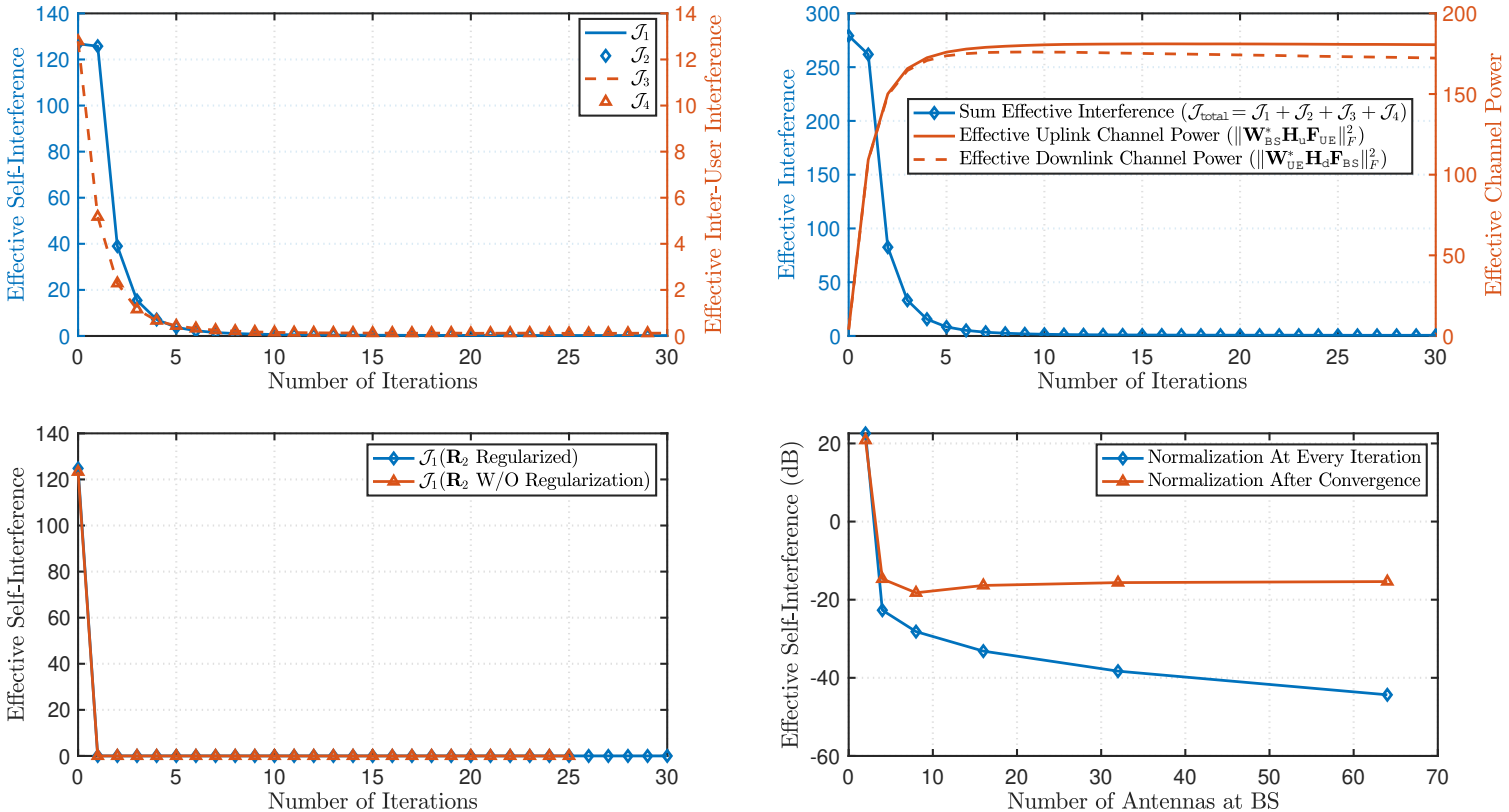

(a) Convergence of the objective functions defining the effective interference in linear scale with respect to the number of iterations. (b) Illustration of the convergence of the sum objective function $\mathcal{J}_{\text{total}} = \mathcal{J}_1 + \mathcal{J}_2 + \mathcal{J}_3 + \mathcal{J}_4$, as well as, the uplink/downlink beamformed/effective channel power. (c) Illustration of the monotonic decreasing of the SI power for $\mathbf{R}_2$ being with/without regularization. (d) Illustration of the effect of beamforming normalization; at every iteration and after the convergence. The plot is produced with $N_{\text{BS}} = 64$, $N_{\text{UE}} = 8$, SNR $= 0$ dB, SI power $\rho_{\text{s}} = 15$ dB and IUI power $\rho_{\text{iui}} = 5$ dB

Contribution 3: Integrated Access and Backhaul

Integrated Access and Backhaul (IAB)

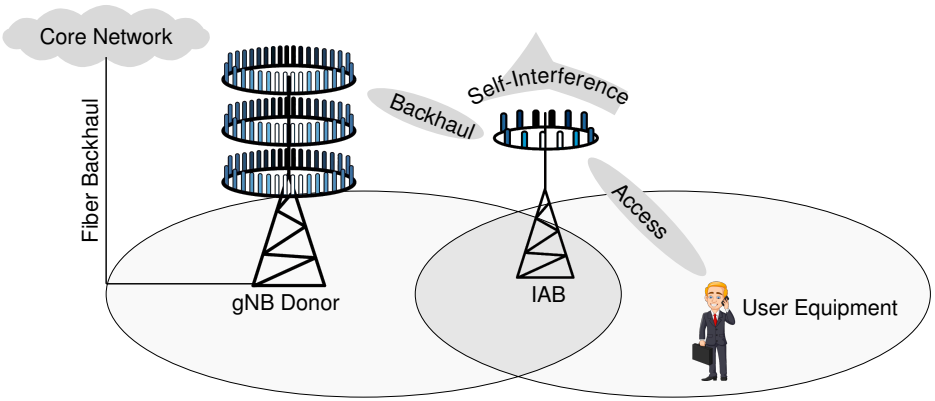

Full-duplex integrated access and backhaul (IAB) for a single-user case. The gNB donor, linked to the core network by fiber backhaul, communicates with the IAB node through wireless backhaul. The user equipment is served by the IAB node through the wireless access link. Simultaneous transmission and reception of the IAB node over the same time/frequency resources blocks incurs loopback self-interference

- The uplink and downlink data are independent
- The backhaul link signal is corrupted by the self-interference
- The access link is interference-free

Hybrid Analog/Digital Abstraction IAB

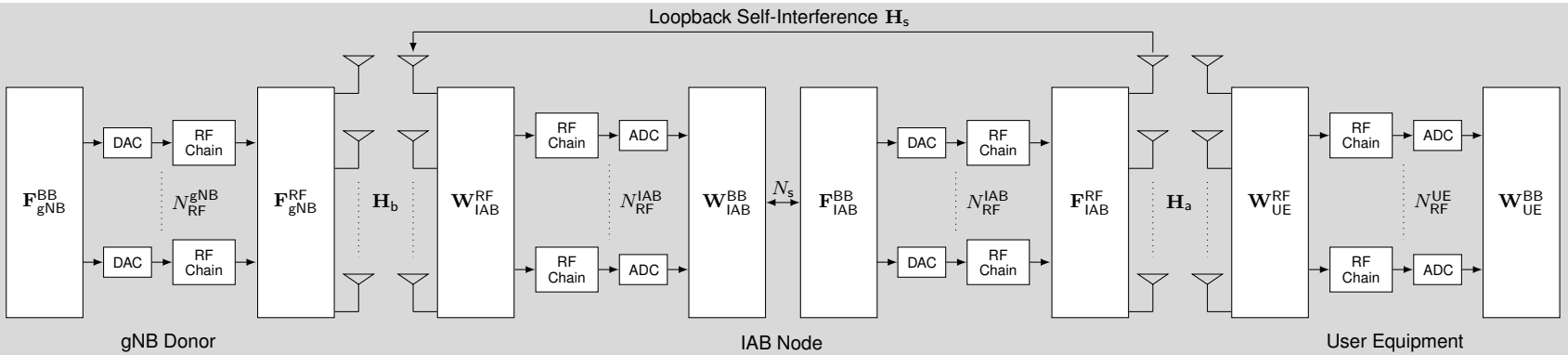

Basic abstraction of the hybrid analog/digital architecture of the full-duplex integrated access and backhaul system. The backhaul channel is between the gNB donor and IAB node, and the access channel is between the IAB node and the user equipment

- The gNB donor communicates with the IAB node through the channel $\mathbf{H_b}$
- The IAB node communicates with the user equipment through the channel $\mathbf{H_a}$
- Loopback self-interference is represented through the channel $\mathbf{H_s}$
- Hybrid beamformers at each node are expressed into an analog $\mathbf{X_{RF}} \in \mathbb{C}^{N_{\mathbf{X}} \times N_{\mathbf{RF}}}$ and digital $\mathbf{X_{BB}} \in \mathbb{C}^{N_{\mathbf{RF}} \times N_{\mathbf{s}}}$ components
- With N_X is the number of antennas at node X, N_{RF} is the number of RF chain and N_s is the number of spatial streams

Signal Model

- The received signal at the IAB ($y_b \in \mathbb{C}^{N_s \times 1}$) is given by

$$y_b = \underbrace{\sqrt{\rho_b} W_{IAB}^* H_b F_{gNB} s_b}_{\text{Desired Signal}} + \underbrace{\sqrt{\rho_s} W_{IAB}^* H_s F_{IAB} s_a}_{\text{Self-Interference Signal}} + \underbrace{W_{IAB}^* n_{IAB}}_{\text{AWGN}} \tag{44}$$

- The received signal at the UE ($y_a \in \mathbb{C}^{N_s \times 1}$) is given by

$$y_a = \underbrace{\sqrt{\rho_a} W_{UE}^* H_a F_{IAB} s_a}_{\text{Desired Signal}} + \underbrace{W_{UE}^* n_{UE}}_{\text{AWGN}} \tag{45}$$

- Where $W_{IAB} \in \mathbb{C}^{N_{IAB} \times N_s}$, $F_{IAB} \in \mathbb{C}^{N_{IAB} \times N_s}$, are the all-digital combiner and precoder at the IAB node, respectively, and $W_{UE} \in \mathbb{C}^{N_{UE} \times N_s}$ and $F_{gNB} \in \mathbb{C}^{N_{gNB} \times N_s}$ are the all-digital combiner and precoder at the UE and gNB node, respectively
- ρ_b, ρ_a and ρ_s are the average transmit powers of backhaul, access and self-interference, respectively
- s_b and s_a are the complex data vectors transmitted through the backhaul and access links, respectively

Hybrid Beamforming

- The main objective is to maximize the sum spectral efficiency of the backhaul and access links
- Propose a two-stage beamforming design: analog and digital.
- Joint beamforming design to simultaneously
  1. Reject the interference
  2. Maintain a spatial multiplexing gain, i.e., preserve the rank of the effective channel ($\mathbf{H}_{\text{eff}} = \mathbf{W}^{*}\mathbf{H}\mathbf{F}$)
- Suppress large amount of SI in analog domain to avoid the ADC saturation
- Residual interference is wiped out in the digital domain

Hybrid Beamforming: Analog Stage

- We aim at minimizing the self-interference power. Equivalently, we define the covariance matrix of the precoded SI and noise at the IAB node as

$$\mathbf{R}_{\mathbf{IAB}} = \rho_s \mathbf{H}_s \mathbf{F}_{\mathbf{IAB}}^{\mathbf{RF}} \mathbf{F}_{\mathbf{IAB}}^{\mathbf{RF}*} \mathbf{H}_s^* + \sigma^2 \mathbf{I}_{N_{\mathbf{IAB}}} \tag{46}$$

- In order to maintain the rank of the effective channel and minimize the SI power, we reformulate the problem as

$$\begin{aligned} \mathscr{P}_1 : \min_{\mathbf{W}_{\mathbf{IAB}}^{\mathbf{RF}}} \ & \mathrm{Tr}\left(\mathbf{W}_{\mathbf{IAB}}^{\mathbf{RF}*} \mathbf{R}_{\mathbf{IAB}} \mathbf{W}_{\mathbf{IAB}}^{\mathbf{RF}}\right) \\ \text{s.t. } & \mathbf{W}_{\mathbf{IAB}}^{\mathbf{RF}*} \mathbf{H}_b \mathbf{F}_{\mathbf{gNB}}^{\mathbf{RF}} = \alpha \mathbf{I}_{N_{\mathbf{RF}}^{\mathbf{IAB}}} \end{aligned} \tag{47}$$

- Equivalently, we define the covariance of the combined SI and noise at the IAB node as

$$\mathbf{S}_{\mathbf{IAB}} = \rho_s \mathbf{H}_s^* \mathbf{W}_{\mathbf{IAB}}^{\mathbf{RF}} \mathbf{W}_{\mathbf{IAB}}^{\mathbf{RF}*} \mathbf{H}_s + \sigma^2 \mathbf{I}_{N_{\mathbf{IAB}}} \tag{48}$$

- Relatively, the second problem can reformulated as

$$\begin{aligned} \mathscr{P}_2 : \min_{\mathbf{F}_{\mathbf{IAB}}^{\mathbf{RF}}} \ & \mathrm{Tr}\left(\mathbf{F}_{\mathbf{IAB}}^{\mathbf{RF}*} \mathbf{S}_{\mathbf{IAB}} \mathbf{F}_{\mathbf{IAB}}^{\mathbf{RF}}\right) \\ \text{s.t. } & \mathbf{W}_{\mathbf{UE}}^{\mathbf{RF}*} \mathbf{H}_a \mathbf{F}_{\mathbf{IAB}}^{\mathbf{RF}} = \beta \mathbf{I}_{N_{\mathbf{RF}}^{\mathbf{IAB}}} \end{aligned} \tag{49}$$

- Note that $\mathbf{R}_{\mathbf{IAB}}$ and $\mathbf{S}_{\mathbf{IAB}}$ are positive definite matrices and α and β are power normalization coefficients

Hybrid Beamforming: Analog Stage

Theorem

- *The optimal analog combiner and precoder at the IAB node, solutions to the problems (47) and (49) are expressed by*

$$W_{IAB}^{RF} = \alpha R_{IAB}^{-1} H_b F_{gNB}^{RF} \left(F_{gNB}^{RF*} H_b^* R_{IAB}^{-1} H_b F_{gNB}^{RF} \right)^{-1} \tag{50}$$

$$F_{IAB}^{RF} = \beta S_{IAB}^{-1} H_a^* W_{UE}^{RF*} \left(W_{UE}^{RF*} H_a S_{IAB}^{-1} H_a^* W_{UE}^{RF} \right)^{-1} \tag{51}$$

Proof.

- Given that problems (47) and (49) are convex, we refer to Lagrange approach to derive the closed-form solutions

□

Hybrid Beamforming: Analog Stage

Theorem

- *The analog combiner at the UE that minimizes the SI and hence the Mean Square Error (MSE) is the Wiener filter or Linear Minimum (LMMSE) receiver* $\mathrm{W}_{\mathrm{MMSE}}$*. The filter design problem can be defined as*

$$\mathscr{P}_3 : \mathrm{W}_{\mathrm{MMSE}} = \min_{\mathrm{W}} \mathbb{E}\left[\|\mathrm{s} - \mathrm{W}^{*}\mathrm{y}\|_2^2\right] \tag{52}$$

- *For the analog precoder at the gNB, we adopt the Regularized Zero-Forcing filter* $\mathrm{F}_{\mathrm{RegZF}}$*. The expressions of the analog combiner and precoder at the UE and gNB, respectively, are given by*

$$\mathrm{W}_{\mathrm{UE}}^{\mathrm{RF}} = \left(\mathrm{H}_{\mathrm{a}}\mathrm{F}_{\mathrm{IAB}}^{\mathrm{RF}}\mathrm{F}_{\mathrm{IAB}}^{\mathrm{RF}*}\mathrm{H}_{\mathrm{a}}^{*} + \frac{N_{\mathrm{UE}}}{\mathrm{SNR}_{\mathrm{a}}}\mathrm{I}_{N_{\mathrm{UE}}}\right)^{-1}\mathrm{H}_{\mathrm{a}}\mathrm{F}_{\mathrm{IAB}}^{\mathrm{RF}} \tag{53}$$

$$\mathrm{F}_{\mathrm{gNB}}^{\mathrm{RF}} = \left(\mathrm{H}_{\mathrm{b}}^{*}\mathrm{W}_{\mathrm{IAB}}^{\mathrm{RF}}\mathrm{W}_{\mathrm{IAB}}^{\mathrm{RF}*}\mathrm{H}_{\mathrm{b}} + \frac{N_{\mathrm{IAB}}}{\mathrm{SNR}_{\mathrm{b}}}\mathrm{I}_{N_{\mathrm{IAB}}}\right)^{-1}\mathrm{H}_{\mathrm{b}}^{*}\mathrm{W}_{\mathrm{IAB}}^{\mathrm{RF}} \tag{54}$$

- The analog beamformers are coupled. Hence an iterative routine is required for the convergence.

Hybrid Beamforming: Digital Stage

Theorem

- *The optimal digital beamformer* X_{BB} *can be expressed in terms of the analog beamformer* X_{RF} *as follows. We first apply the SVD* $\mathsf{X}_{\mathsf{RF}} = \mathsf{U}_{\mathsf{RF}}\mathsf{S}_{\mathsf{RF}}\mathsf{V}_{\mathsf{RF}}^{*}$*. Second we express* $\mathsf{X}_{\mathsf{BB}} = \mathsf{V}_{\mathsf{RF}}\mathsf{S}_{\mathsf{RF}}^{-1}\mathsf{Q}_{\star}$*, where the columns of* $\mathsf{Q}_{\star} \in \mathbb{C}^{M \times N}$ *comprise the* N *dominant left singular vectors of* $\mathsf{U}_{\mathsf{RF}}^{*}\mathsf{A}$*. Note that* $\mathsf{X}_{\mathsf{RF}} \in \mathbb{C}^{M \times L}$*,* $\mathsf{X}_{\mathsf{BB}} \in \mathbb{C}^{L \times N}$ *and* $\mathsf{A} \in \mathbb{C}^{M \times N}$

Convergence

- We define the effective self-interference as

$$\mathcal{J} = \mathrm{Tr}\left(\rho_{\mathbf{s}} \mathbf{W}_{\mathbf{IAB}}^{\mathbf{RF}*} \mathbf{H}_{\mathbf{s}} \mathbf{F}_{\mathbf{IAB}}^{\mathbf{RF}} \mathbf{F}_{\mathbf{IAB}}^{\mathbf{RF}*} \mathbf{H}_{\mathbf{s}}^{*} \mathbf{W}_{\mathbf{IAB}}^{\mathbf{RF}}\right) \tag{55}$$

- Algorithm converges in a few iterations
- Analog beamforming drops the SI power from 128 to 16 to prevent the ADC saturation (8x)
- Digital beamforming drops the SI power from 16 to 10.06 (1.5x)

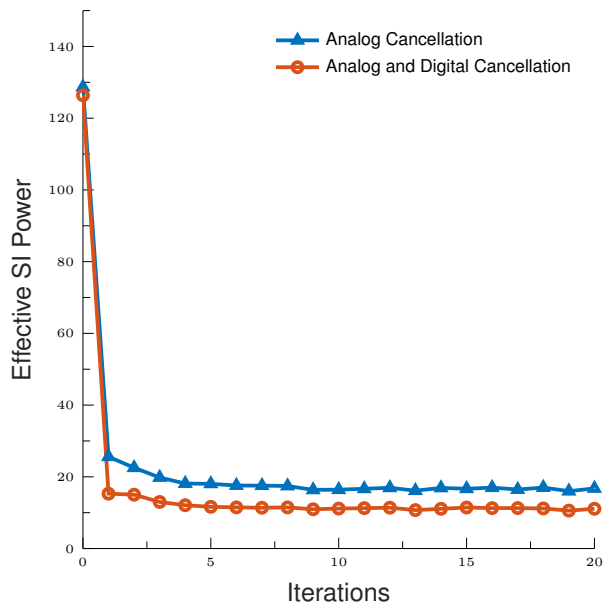

Convergence of the cost function $\mathcal{J}$ defined in (55). The plot is produced with $\mathbf{SNR} = \mathbf{0\ dB}$ and SI power $\rho_{\mathbf{s}} = \mathbf{15\ dB}$

Complexity Analysis

Table 5: Computational complexity of the hybrid beamforming algorithm. Parameters values are selected from Table 6

Operation	Complex Multiplications for Highest-Order Terms	Flops	Dominant Term	Contribution (Total)
W_{IAB}^{RF}	$\frac{3}{2}N_{IAB}^2 N_{RF}^{IAB} + \frac{1}{3}N_{IAB}^3 + N_{gNB}N_{IAB}N_{RF}^{gNB} + \frac{1}{3}\left(N_{RF}^{gNB}\right)^3 + N_{IAB}^2 N_{RF}^{gNB}$	21165	$\frac{1}{3}N_{IAB}^3$	51.61% (16.06%)
F_{IAB}^{RF}	$\frac{3}{2}N_{IAB}^2 N_{RF}^{IAB} + \frac{1}{3}N_{IAB}^3 + N_{UE}N_{IAB}N_{RF}^{UE} + \frac{1}{3}\left(N_{RF}^{UE}\right)^3 + N_{IAB}^2 N_{RF}^{UE}$	19373	$\frac{1}{3}N_{IAB}^3$	56.38% (16.06%)
F_{gNB}^{RF}	$\frac{3}{2}N_{gNB}^2 N_{RF}^{gNB} + \frac{1}{3}N_{gNB}^3$	13995	$\frac{1}{3}N_{gNB}^3$	78.05% (16.06%)
W_{IAB}^{BB}	$9\left(N_{RF}^{IAB}\right)^2 N_{IAB} + 9N_s^2 N_{IAB} + N_{IAB}^2 N_s + N_s^3$	4360	$N_{IAB}^2 N_s$	46.97% (3.03%)
F_{IAB}^{BB}	$9\left(N_{RF}^{IAB}\right)^2 N_{IAB} + 9N_s^2 N_{IAB} + N_{IAB}^2 N_s + N_s^3$	4360	$N_{IAB}^2 N_s$	46.97% (3.01%)
F_{gNB}^{BB}	$9\left(N_{RF}^{gNB}\right)^2 N_{gNB} + 9N_s^2 N_{gNB} + N_{gNB}^2 N_s + N_s^3$	4360	$N_{gNB}^2 N_s$	46.97% (3.01%)
W_{UE}^{BB}	$9\left(N_{RF}^{UE}\right)^2 N_{UE} + 9N_s^2 N_{UE} + N_{UE}^2 N_s + N_s^3$	328	$9\left(N_{RF}^{UE}\right)^2 N_{UE}$	43.90% (0.21%)
W_{UE}^{RF}	$\frac{3}{2}N_{UE}^2 N_{RF}^{UE} + \frac{1}{3}N_{UE}^3$	70	$\frac{3}{2}N_{UE}^2 N_{RF}^{UE}$	69.23% (0.07%)

Performance Measures

- The spectral efficiency for the backhaul and access links, respectively, are

$$\mathcal{I}_{\mathsf{b}} = \log\det\left(\mathsf{I}_{N_{\mathsf{s}}} + \rho_{\mathsf{b}}\mathsf{W}_{\mathsf{IAB}}^{*}\mathsf{H}_{\mathsf{b}}\mathsf{F}_{\mathsf{gNB}}\mathsf{Q}_{\mathsf{b}}^{-1}\mathsf{F}_{\mathsf{gNB}}^{*}\mathsf{H}_{\mathsf{b}}^{*}\mathsf{W}_{\mathsf{IAB}}\right) \tag{56}$$

$$\mathcal{I}_{\mathsf{a}} = \log\det\left(\mathsf{I}_{N_{\mathsf{s}}} + \rho_{\mathsf{a}}\mathsf{W}_{\mathsf{UE}}^{*}\mathsf{H}_{\mathsf{a}}\mathsf{F}_{\mathsf{IAB}}\mathsf{Q}_{\mathsf{a}}^{-1}\mathsf{F}_{\mathsf{IAB}}^{*}\mathsf{H}_{\mathsf{a}}^{*}\mathsf{W}_{\mathsf{UE}}\right) \tag{57}$$

- Where Q_{b} is the covariance matrix of the SI and noise power for the backhaul link and Q_{a} is the covariance matrix of the noise power for the access link, respectively, given by

$$\mathsf{Q}_{\mathsf{b}} = \rho_{\mathsf{s}}\mathsf{W}_{\mathsf{IAB}}^{*}\mathsf{H}_{\mathsf{s}}\mathsf{F}_{\mathsf{IAB}}\mathsf{F}_{\mathsf{IAB}}^{*}\mathsf{H}_{\mathsf{s}}^{*}\mathsf{W}_{\mathsf{IAB}} + \sigma^{2}\mathsf{W}_{\mathsf{IAB}}^{*}\mathsf{W}_{\mathsf{IAB}} \tag{58}$$

$$\mathsf{Q}_{\mathsf{a}} = \sigma^{2}\mathsf{W}_{\mathsf{IAB}}^{*}\mathsf{W}_{\mathsf{IAB}} \tag{59}$$

Lemma

- *For the interference-free case, the optimal beamformers diagonalize the channel. By applying the SVD on the channel, we retrieve the singular values and extract the first N_{s} modes associated with the spatial streams. The upper bound for backhaul or access link is given by*

$$\mathcal{I}_{\mathsf{Bound}} = \sum_{\ell=0}^{N_{\mathsf{s}}-1} \log\left(1 + \sigma_{\ell}\left(\mathsf{H}\right)^{2}\mathsf{SNR}\right) \tag{60}$$

Numerical Results

Table 6: System Parameters

Parameter	**Value**
Carrier frequency	28 GHz
Bandwidth	850 MHz
Number of gNB/IAB Antennas ($N_{\text{gNB}}/N_{\text{IAB}}$)	32
Number of UE Antennas (N_{UE})	4
Number of Clusters (C)	6
Number of Rays per Cluster (R_c)	8
AoA/AoD Angular Spread	20°
Transceivers Gap (d)	2λ
Transceivers Incline (ω)	$\frac{\pi}{6}$
Rician Factor (κ)	5 dB
SI Power (ρ_{s})	15 dB
Number of Spatial Streams (N_{s})	2
Number of RF Chains (N_{RF})	2

Numerical Analysis

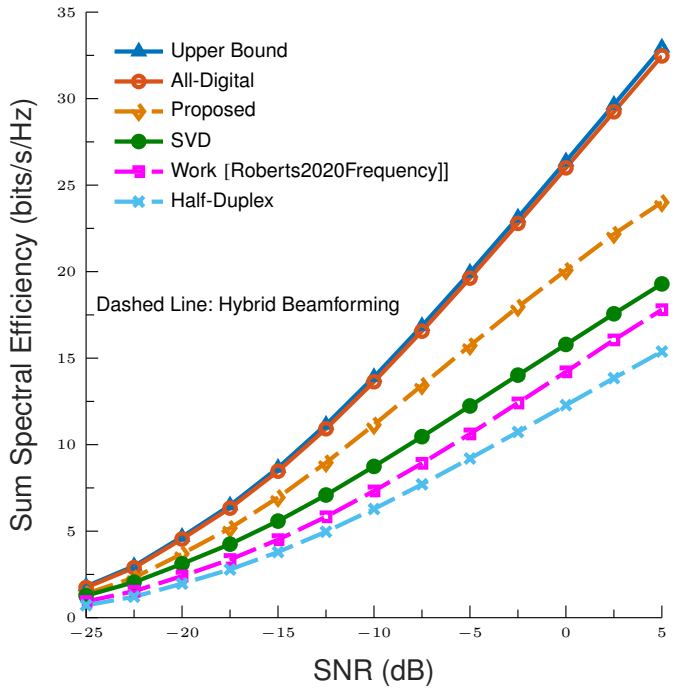

Sum spectral efficiency results: Performance comparison between the proposed algorithm with the related works as well as the benchmarking tools

- Proposed beamforming design still suffers from residual SI power
- Proposed design beats related work as well as the half-duplex mode

---

Ian P. Roberts, Hardik B. Jain, and Sriram Vishwanath. Frequency-Selective Beamforming Cancellation Design for Millimeter-Wave Full-Duplex. In: *IEEE International Conference on Communications (ICC)*. 2020, pp. 1–6.

Contribution #3: Integrated Access and Backhaul

1. Considered FD based integrated accecss and backhaul systems
   - Full-digital beamformers
   - Hybrid analog/digital beamformers
   - Self-interference
2. Complexity Analysis
   - Low computational cost
   - Convergence in a few iterations
3. Designed full-digital and hybrid analog/digital beamformers
   - Used degrees of freedom due to massive number of antennas
   - Cancel the interference and maintain spatial multiplexing gain
4. Full duplex system outperforms half-duplex mode in sum spectral efficiency
   - Gives evidence of feasibility of FD systems in the integrated access and backhaul scenario

Contribution 4: Multiuser MIMO

Convergence

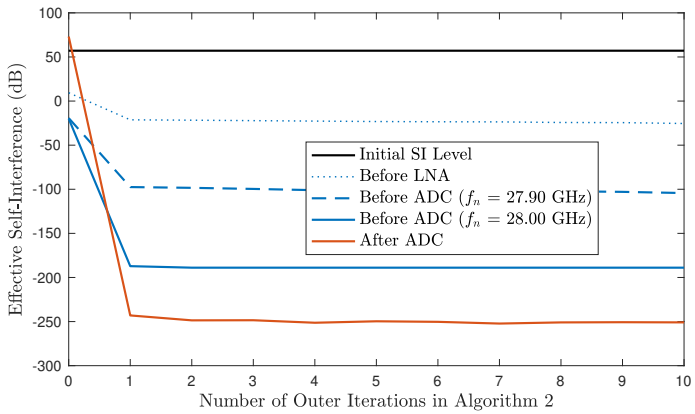

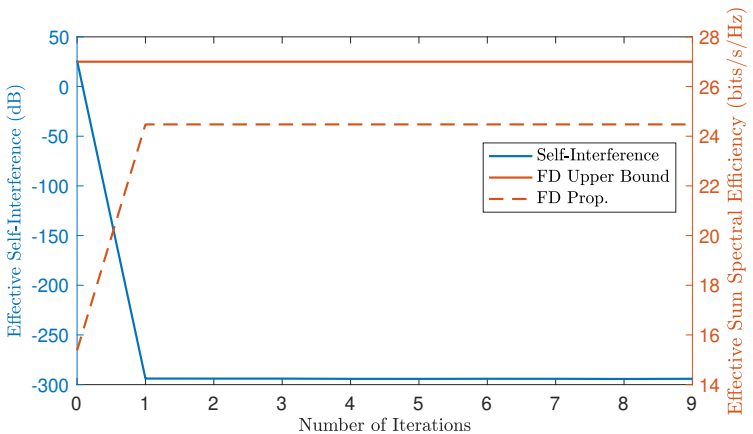

Illustration of the global convergence of Algorithm 2 in terms of SI suppression and sum spectral efficieny vs. number of iterations. The considered system parameters are: 10 inner iterations in Algorithm 2, $\mathcal{N}_{\mathbf{freq}} = 5$, $K = U = 2$, 2 TX/RX RF chains at the BS and each sub-array is equipped with 32 antennas, while each user is equipped with 8 antennas. (a) For the SI suppression evaluated before ADC, we consider two subcarriers; $f_n = 28.00$ GHz where $n \in \{n_1, \ldots, n_{\mathcal{N}_{\mathbf{freq}}}\}$ and $f_n = 27.90$ GHz with $n \notin \{n_1, \ldots, n_{\mathcal{N}_{\mathbf{freq}}}\}$. (b) Results are averaged over all the subcarriers, i.e., across the entire bandwidth

- Fast convergence in 1-2 iterations
- Optimization problem (cost function and constraints) are satisfied:
  1. Effective SI is reduced across the entire system block
  2. Sum rate reaches the maximum leaving a lower gap with the upper bound

Quantized Phase Shifter

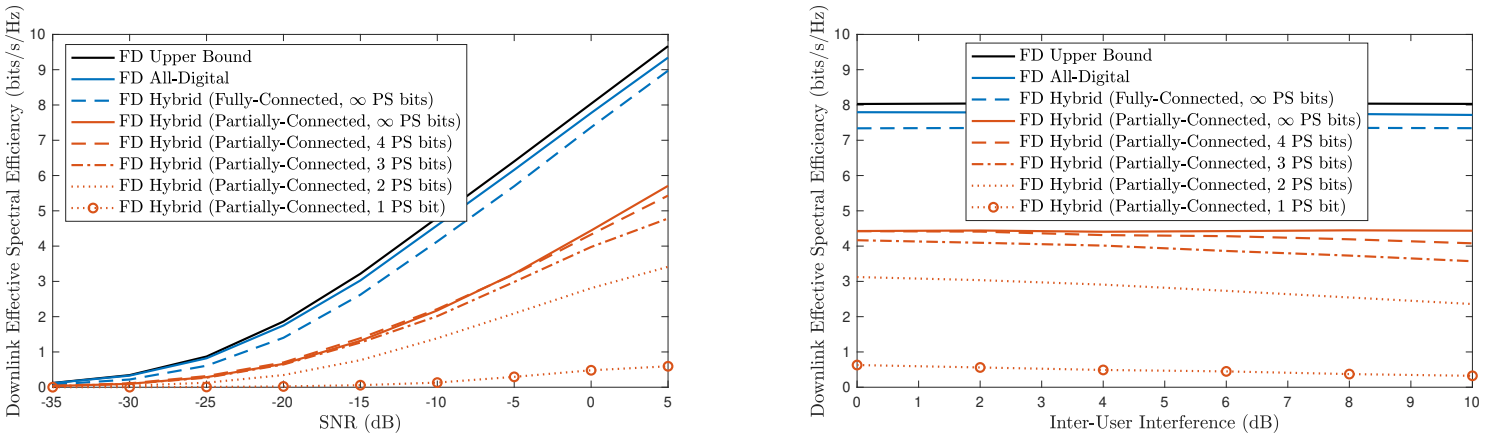

Illustration of the per-user downlink effective spectral efficiency for different phases shifters resolution at the BS and users. (a). Results are obtained with $U = K = 2$ users and an average IUI of 5 **dB** while varying the average SNR. (b). Results are achieved with $U = K = 2$ users and an average SNR of 0 **dB** while varying the average IUI. Note that the BS is equipped with 2 TX/RX RF chains and each sub-array (for partially-connected structure) is equipped with 64 antennas, while each user is equipped with 8 antennas. Note that the IUI is incurred by the uplink users to corrupt the downlink users since the communications (uplink/downlink) occur at the same frequency band

- Performance degrades with lower # bits of phase shifter
- 4 bits are sufficient to achieve near ∞ resolution results

Contribution 5: Massive MIMO Cellular Networks

Introduction

1. Multi-antenna systems reduce hefty power consumption by reducing
   - Number of RF processing chains using hybrid analog/digital beamforming
   - Data converter resolution
2. Solution for full-duplex multiantenna basestation with low-resolution converters
   - Use degrees of freedom in the all-digital beamformer design due to number of antennas to suppress interference
3. Contributions
   - Provide unified framework for cellular reverse and forward links
   - Derive signal to quantization plus interference plus noise ratio (sqinr)
   - Quantify effects on outage probability and spectral efficiency due to
     - Quantization error
     - Pilot contamination
     - Self-interference
     - Inter-user interference
     - Number of users
     - Overhead

Description

1. Network topology: Hexagonal, square and PPP tessellation.
2. Cellular systems (multicell and multiuser)
3. BSs and UEs operate in FD and Half-Duplex (HD), respectively.
4. Massive number of antennas $N_a \gg 1$ at the BS and UEs are equipped with a single antenna
5. BSs operate in low-resolution ADC/DAC
6. Additive Quantization Noise Model (AQNM): $y_q = \alpha y + q$
7. Large-scale fading: Pathloss and Lognormal shadowing
8. Small-scale fading: Rayleigh and geometric channel models
9. Matched filter precoder/receiver at the BS
10. CSI acquisition: LMMSE channel estimation and channel hardening

Visual Abstract

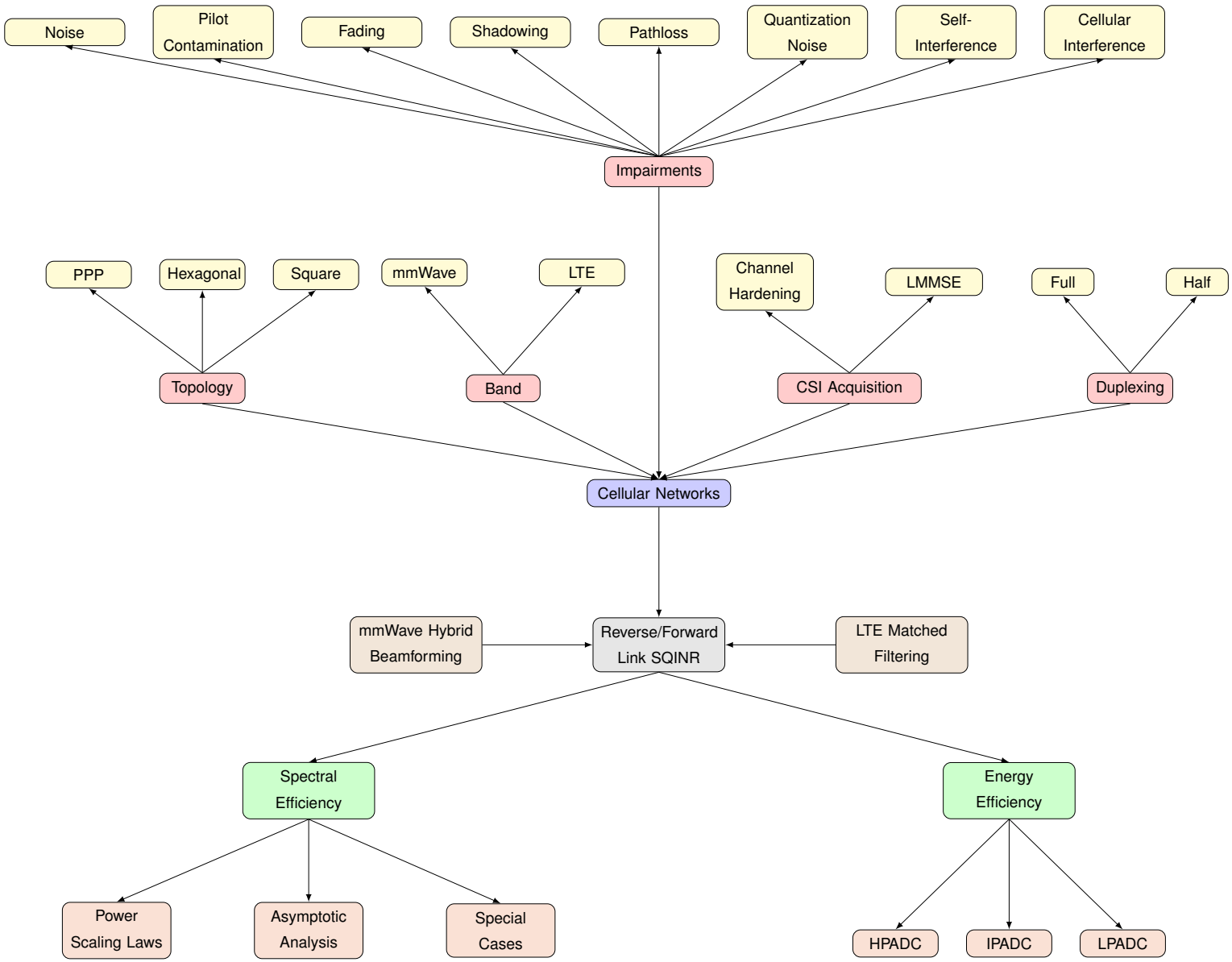

Description

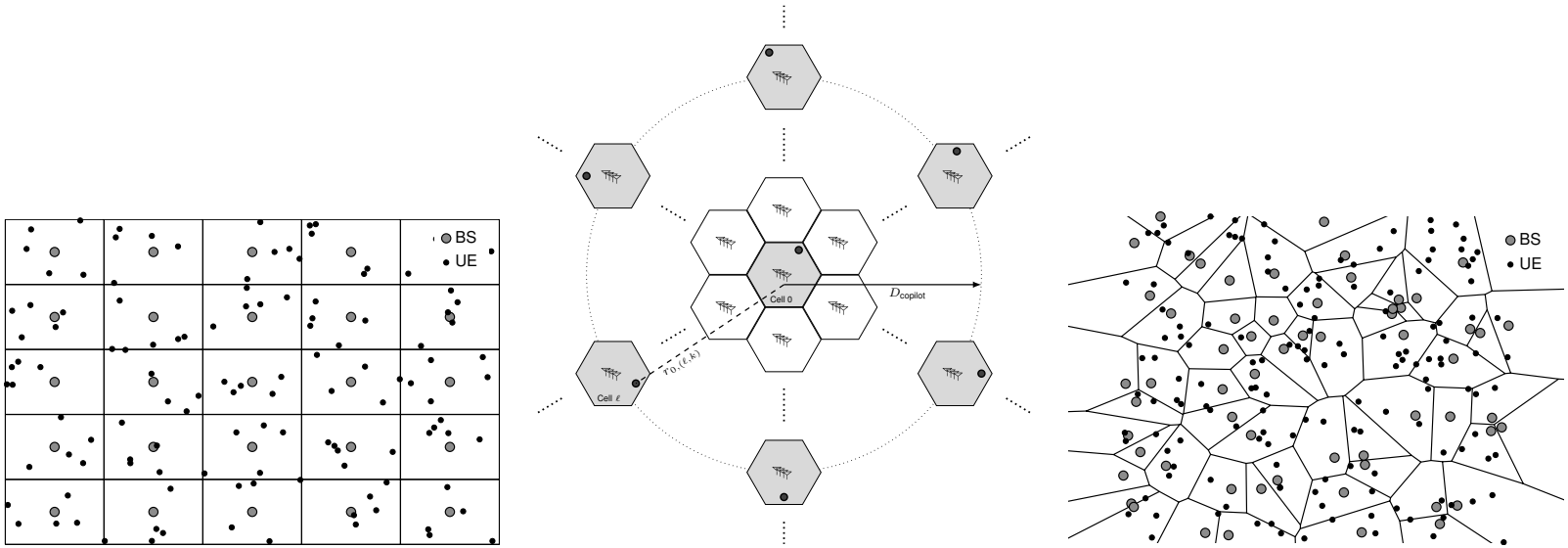

(a) Square grid. (b) Hexagonal lattice. (c) Poisson Point Process (PPP) tessellation

---

Elyes Balti and Brian L. Evans. A Unified Framework for Full-Duplex Massive MIMO Cellular Networks With Low Resolution Data Converters. In: *IEEE Open Journal of the Communications Society* 4 (2023), pp. 1–28.

Elyes Balti and Brian L. Evans. Full-Duplex Massive MIMO Cellular Networks with Low Resolution ADC/DAC. In: *IEEE Global Communications Conference (GLOBECOM)*. 2022, pp. 1649–1654.

Elyes Balti and Brian L. Evans. Reverse Link Analysis for Full-Duplex Cellular Networks with Low Resolution ADC/DAC. In: *2022 IEEE Int. Workshop Signal Process. Adv. Wirel. Commun. (SPAWC)*. 2022, pp. 1–5.

Elyes Balti and Brian L. Evans. Forward Link Analysis for Full-Duplex Cellular Networks with Low Resolution ADC/DAC. In: *2022 IEEE Int. Workshop Signal Process. Adv. Wirel. Commun. (SPAWC)*. 2022, pp. 1–5.

Model

- Large-Scale Fading: Pathloss and Lognormal Shadowing

$$G_{\ell,(l,k)} = \frac{L_{\text{ref}}}{r_{\ell,(l,k)}^{\eta}} \chi_{\ell,(l,k)} \tag{61}$$

- Small-Scale Fading: Rayleigh
- Low-resolution data converters and AQNM

$$\mathsf{y_q} = \alpha \mathsf{y} + \mathsf{q} \tag{62}$$

- For $b \leq 5$, $\rho = 1 - \alpha$ values is given by Table 7

Table 7: ρ for different values of b

b	1	2	3	4	5
ρ	0.3634	0.1175	0.03454	0.009497	0.002499

- Otherwise, ρ can be approximated by

$$\rho \approx \frac{\pi\sqrt{3}}{2} \cdot 2^{-2b} \tag{63}$$

ρ is the inverse of the signal-to-quantization noise ratio

Li Fan, Shi Jin, Chao-Kai Wen, and Haixia Zhang. Uplink Achievable Rate for Massive MIMO Systems With Low-Resolution ADC. In: *IEEE Commun. Let.* 19.12 (2015), pp. 2186–2189.

Signal Model

- The received signal of the k-th uplink user at the BS is given by

$$y_{q,k}^{u} = \underbrace{\alpha_u \sqrt{G_k P_k}\mathbb{E}[\boldsymbol{w}_k^* \boldsymbol{h}_k] s_k}_{\text{Desired Signal}} + \underbrace{\alpha_u \sum_{\mathrm{k}\neq k} \sqrt{G_{\mathrm{k}} P_{\mathrm{k}}} \boldsymbol{w}_k^* \boldsymbol{h}_{\mathrm{k}} s_{\mathrm{k}}}_{\text{Intra-Cell Interference}} + \underbrace{\alpha_u \boldsymbol{w}_k^* \boldsymbol{v}}_{\text{Filtered Noise}}$$

$$\overbrace{+ \underbrace{\alpha_u \sqrt{G_k P_k}\left(\boldsymbol{w}_k^* \boldsymbol{h}_k - \mathbb{E}[\boldsymbol{w}_k^* \boldsymbol{h}_k]\right) s_k}_{\text{Channel Estimation Error}} + \underbrace{\alpha_u \alpha_d \sqrt{P_{\mathrm{SI}}} \sum_{\mathrm{k}=0}^{K^d-1} \boldsymbol{w}_k^* \boldsymbol{H}_{\mathrm{SI}} \boldsymbol{f}_{\mathrm{k}} s_{\mathrm{k}}^d}_{\text{Self-Interference due to Full-Duplexing}}}^{\text{Aggregate Self-Interference}} + \tag{64}$$

$$\underbrace{\alpha_u \sqrt{P_{\mathrm{SI}}} \boldsymbol{w}_k^* \boldsymbol{H}_{\mathrm{SI}} \boldsymbol{q}_d + \boldsymbol{w}_k^* \boldsymbol{q}_u}_{\text{Aggregate AQNM}} + \underbrace{\alpha_u \sum_{\ell\neq 0} \sum_{\mathrm{k}=0}^{K_\ell^u-1} \sqrt{G_{\ell,\mathrm{k}} P_{\ell,\mathrm{k}}} \boldsymbol{w}_k^* \boldsymbol{h}_{\ell,\mathrm{k}} s_{\ell,\mathrm{k}}}_{\text{Inter-Cell Interference}}$$

- The matched filter receiver $\boldsymbol{w}_k^{\mathrm{MF}}$ satisfies the following properties:
  1. $\mathbb{E}\left[\|\boldsymbol{w}_k^{\mathrm{MF}}\|^2\right] = N_{\mathrm{a}}$
  2. $\mathbb{E}\left[\|\boldsymbol{w}_k^{\mathrm{MF}}\|^4\right] = N_{\mathrm{a}}^2 + N_{\mathrm{a}}$
  3. $\mathbb{E}\left[\left|\boldsymbol{w}_k^{\mathrm{MF}*} \boldsymbol{h}_{\ell,\mathrm{k}}\right|^2\right] = N_{\mathrm{a}}$

Uplink SQINR

Theorem

The output SQINR of the k-th uplink user is given by

$$\overline{\text{sqinr}}_k^{\text{MF}} = \frac{\alpha_u^2 G_k P_k \left|\mathbb{E}[\boldsymbol{w}_k^{\text{MF}*} \boldsymbol{h}_k]\right|^2}{\overline{\text{den}}_u^{\text{MF}}} \tag{65}$$

where $\overline{\text{den}}_u^{\text{MF}}$ *is given by*

$$\begin{aligned}\overline{\text{den}}_u^{\text{MF}} &= \alpha_u^2 G_k P_k \text{var}[\boldsymbol{w}_k^{\text{MF}*} \boldsymbol{h}_k] + \alpha_u^2 \sum_{k \neq k} G_k P_k \mathbb{E}\left[\left|\boldsymbol{w}_k^{\text{MF}*} \boldsymbol{h}_k\right|^2\right] + \alpha_u^2 \sigma^2 \mathbb{E}\left[\left\|\boldsymbol{w}_k^{\text{MF}}\right\|^2\right] \\ &+ \alpha_u^2 \sum_{\ell \neq 0} \sum_{k=0}^{K_\ell^d - 1} G_{\ell,k} P_{\ell,k} \mathbb{E}\left[\left|\boldsymbol{w}_k^{\text{MF}*} \boldsymbol{h}_{\ell,k}\right|^2\right] + \alpha_u^2 \alpha_d^2 P_{\text{SI}} \sum_{k=0}^{K^d - 1} \mathbb{E}\left[\left|\boldsymbol{w}_k^{\text{MF}*} \boldsymbol{H}_{\text{SI}} \boldsymbol{f}_k^{\text{MF}}\right|^2\right] \\ &+ \alpha_u^2 P_{\text{SI}} \mathbb{E}\left[\left|\boldsymbol{w}_k^{\text{MF}*} \boldsymbol{H}_{\text{SI}} \boldsymbol{q}_d\right|^2\right] + \mathbb{E}\left[\left|\boldsymbol{w}_k^{\text{MF}*} \boldsymbol{q}_u\right|^2\right]\end{aligned} \tag{66}$$

Special Cases

Corollary

To further characterize the spectral efficiency, we derive a new bound using the following formula. Assuming statistical independence between x and y, we have

$$\mathbb{E}\left[\log\left(1+\frac{x}{y}\right)\right] \cong \log\left(1+\frac{\mathbb{E}[x]}{\mathbb{E}[y]}\right)$$

Proposition

Considering a single-cell multiuser system (without any inter-cell interference) with perfect CSI, Corollary (above) entails the results for reverse link in[a]

[a] Jianxin Dai, Juan Liu, Jiangzhou Wang, Junxi Zhao, Chonghu Cheng, and Jin-Yuan Wang. Achievable Rates for Full-Duplex Massive MIMO Systems With Low-Resolution ADCs/DACs. In: *IEEE Access* 7 (2019), pp. 24343–24353.

Signal Model

- The received signal of the k-th downlink user is given by

$$y_{q,k}^{d} = \underbrace{\alpha_d \sqrt{\frac{G_k P_k}{N_{\mathrm{a}}}} \mathbb{E}[\boldsymbol{h}_k^* \boldsymbol{f}_k] s_k}_{\text{Desired Signal}} + \underbrace{\alpha_d \sqrt{\frac{G_k P_k}{N_{\mathrm{a}}}} \left(\boldsymbol{h}_k^* \boldsymbol{f}_k - \mathbb{E}[\boldsymbol{h}_k^* \boldsymbol{f}_k]\right) s_k}_{\text{Channel Estimation Error (Self-Interference)}}$$

$$+ \underbrace{\alpha_d \sum_{\mathrm{k} \neq k} \sqrt{\frac{G_k P_{\mathrm{k}}}{N_{\mathrm{a}}}} \boldsymbol{h}_k^* \boldsymbol{f}_{\mathrm{k}} s_{\mathrm{k}}}_{\text{Intra-Cell Interference}} + \underbrace{\sum_{\ell} \sum_{\mathrm{k}=0}^{K_\ell^d - 1} \sqrt{\frac{G_{\ell,k} P_{\ell,\mathrm{k}}}{N_{\mathrm{a}}}} \boldsymbol{h}_{\ell,k}^* \boldsymbol{q}_\ell}_{\text{Aggregate AQNM}} + \underbrace{\sum_{\mathrm{k} \neq k} \sqrt{T_{\mathrm{k},k} P_{\ell,\mathrm{k}}^u} \boldsymbol{g}_{\mathrm{k},k} s_{\mathrm{k},u}}_{\text{Same Cell Inter-User Interference}}$$

$$+ \underbrace{\alpha_d \sum_{\ell \neq 0} \sum_{\mathrm{k}=0}^{K_\ell^d - 1} \sqrt{\frac{G_{\ell,k} P_{\ell,\mathrm{k}}}{N_{\mathrm{a}}}} \boldsymbol{h}_{\ell,k}^* \boldsymbol{f}_{\ell,\mathrm{k}} s_{\ell,\mathrm{k}}}_{\text{Inter-Cell Interference}} + \underbrace{\sum_{\ell \neq 0} \sum_{\mathrm{k}=0}^{K_\ell^u - 1} \sqrt{T_{(\ell,\mathrm{k}),k} P_{\ell,\mathrm{k}}^u} \boldsymbol{g}_{(\ell,\mathrm{k}),k} s_{\ell,\mathrm{k},u}}_{\text{Other Cells Inter-User Interference}} + \underbrace{v_k}_{\text{Noise}} \tag{67}$$

- The matched filter precoder $\boldsymbol{f}_k^{\mathrm{MF}}$ satisfies the following properties:
  1. $\mathbb{E}\left[\|\boldsymbol{f}_k^{\mathrm{MF}}\|^2\right] = N_{\mathrm{a}}$
  2. $\mathbb{E}\left[\|\boldsymbol{f}_k^{\mathrm{MF}}\|^4\right] = N_{\mathrm{a}}^2 + N_{\mathrm{a}}$
  3. $\mathbb{E}\left[\left|\boldsymbol{h}_{\ell,\mathrm{k}}^* \boldsymbol{f}_k^{\mathrm{MF}}\right|^2\right] = N_{\mathrm{a}}$

Downlink SQINR

Theorem

The output SQINR of the k-th downlink user is given by

$$\overline{\text{sqinr}}_k^{\text{MF}} = \frac{\alpha_d^2 \frac{G_k P_k}{N_{\text{a}}} \left| \mathbb{E}\left[\boldsymbol{h}_k^* \boldsymbol{f}_k^{\text{MF}} \right] \right|^2}{\overline{\text{den}}_d^{\text{MF}}} \tag{68}$$

where $\overline{\text{den}}_d^{\text{MF}}$ *is given by (69).*

$$\begin{aligned}
\overline{\text{den}}_d^{\text{MF}} &= \alpha_d^2 \frac{G_k P_k}{N_{\text{a}}} var\left[\boldsymbol{h}_k^* \boldsymbol{f}_k^{\text{MF}} \right] + \alpha_d^2 \sum_{k \neq k} \frac{G_k P_k}{N_{\text{a}}} \mathbb{E}\left[\left| \boldsymbol{h}_k^* \boldsymbol{f}_k^{\text{MF}} \right|^2 \right] + \sum_{k \neq k} T_{k,k} P_k^u \mathbb{E}\left[\left| \boldsymbol{g}_{k,k} \right|^2 \right] \\
&+ \alpha_d^2 \sum_{\ell \neq 0} \sum_{k=0}^{K_\ell^d - 1} \frac{G_{\ell,k} P_{\ell,k}}{N_{\text{a}}} \mathbb{E}\left[\left| \boldsymbol{h}_{\ell,k}^* \boldsymbol{f}_{\ell,k}^{\text{MF}} \right|^2 \right] + \sum_{\ell \neq 0} \sum_{k=0}^{K_\ell^u - 1} T_{(\ell,k),k} P_{\ell,k}^u \mathbb{E}\left[\left| \boldsymbol{g}_{(\ell,k),k} \right|^2 \right] \\
&+ \sum_{\ell} \frac{G_{\ell,k} P_{\ell,k}}{N_{\text{a}}} \mathbb{E}\left[\left| \boldsymbol{h}_{\ell,k}^* \boldsymbol{q}_\ell \right|^2 \right] + \sigma^2
\end{aligned} \tag{69}$$

Special Cases

Proposition

Considering a single-cell multiuser system (without any inter-cell interference) with perfect CSI, Corollary (in reverse link section) entails the results for downlink users in[a]

[a] Jianxin Dai, Juan Liu, Jiangzhou Wang, Junxi Zhao, Chonghu Cheng, and Jin-Yuan Wang. Achievable Rates for Full-Duplex Massive MIMO Systems With Low-Resolution ADCs/DACs. In: *IEEE Access* 7 (2019), pp. 24343–24353.

Proposition

For channel hardening without full-duplexing (hence no co-channel interference between users) and with full-resolution ADC/DACs, we retrieve the results derived for downlink users in multicell massive MIMO systems in[a]

[a] Geordie George, Angel Lozano, and Martin Haenggi. Massive MIMO Forward Link Analysis for Cellular Networks. In: *IEEE Transactions on Wireless Communications* 18.6 (June 2019), pp. 2964–2976.

Effects of Data Converters Resolution

Lemma

For a fixed power budget, fixed number of transmit antennas and full-resolution ($b \to \infty$, $\alpha_u = \alpha_d = 1$), the spectral efficiencies for reverse and forward links converge to

$$\frac{\bar{\mathcal{I}}_k^u}{B} \to \log\left(1 + \frac{G_k P_k N_{\mathsf{a}}}{\sum_\ell \sum_k G_{\ell,k} P_{\ell,k} + P_{\mathsf{SI}} \mu_{\mathsf{SI}}^2 K^d N_{\mathsf{a}} + \sigma^2}\right) \tag{70}$$

$$\frac{\bar{\mathcal{I}}_k^d}{B} \to \log\left(1 + \frac{G_k P_k}{\sum_\ell \sum_k G_{\ell,k} P_{\ell,k} + \sum_\ell \sum_k T_{(\ell,k),k} P_{\ell,k}^u \sigma_{\mathsf{iui}}^2 + \sigma^2}\right) \tag{71}$$

- With fixed number of antennas, the spectral efficiency is constant
- Through increasing ADC/DAC resolution to enhance the performance, the spectral efficiency is limited

Effects of Transmit Power

Lemma

For a fixed number of antennas, fixed b and when $P_{\mathsf{SI}} = P^d = P^u \to \infty$, the spectral efficiency converges to

$$\frac{\bar{\mathcal{I}}_k^u}{B} \to \log\left(1 + \frac{\alpha_u G_k N_{\mathsf{a}}}{\sum_\ell \sum_k G_{\ell,k} + (1-\alpha_u) G_k + \alpha_d N_{\mathsf{a}} \mu_{\mathsf{SI}}^2 \left[1 + \alpha_u \alpha_d (K^d - 1)\right]}\right) \tag{72}$$

$$\frac{\bar{\mathcal{I}}_k^d}{B} \to \log\left(1 + \frac{\alpha_d^2 G_k}{\alpha_d^2 \sum_\ell \sum_k G_{\ell,k} + \sum_\ell \sum_k T_{(\ell,k),k} \sigma_{\mathsf{iui}}^2 + \alpha_d (1-\alpha_d) \sum_\ell G_{\ell,k} (K_\ell^d + 1)}\right) \tag{73}$$

- The spectral efficiency depends on the number of antennas and quantization bits
- Uplink and downlink spectral efficiencies are saturated by a ceiling caused by SI, IUI powers and quantization error, respectively

Power Scaling Laws

Lemma

If the transmit powers of the BS and each user is scaled with the number of antennas N_a i.e., $P = \frac{E}{N_a}$ where E is fixed, as $N_a \to \infty$, the spectral efficiency converges to

$$\frac{\bar{\mathcal{I}}_k^u}{B} \to \log\left(1 + \frac{\alpha_u G_k E_k}{\alpha_d \mu_{SI}^2 E_{SI}\left[1 + \alpha_u \alpha_d (K^d - 1)\right] + \sigma^2}\right) \tag{74}$$

$$\frac{\bar{\mathcal{I}}_k^d}{B} \to \log\left(1 + \frac{\alpha_d^2 G_k E_k}{\sigma^2}\right) \tag{75}$$

- More antennas can eliminate intra-cell and inter-cell interference for uplink scenario
- More antennas can eliminate the inter-user interference caused by full-duplexing for downlink scenario
- The number of quantization bits determines the approximate uplink and downlink spectral efficiencies when the number of the antennas at a FD BS, N_a, goes to infinity

Performance Measures

- The effective spectral efficiency of the k-th uplink UE is given by

$$\frac{\mathcal{I}_k^{\text{eff}}}{B} = \log\left(1 + \overline{\text{sqinr}}_k\right), \; k = 0, \ldots, K-1$$

- Once a transmission strategy is specified, the corresponding cumulative distribution function (CDF) or outage probability for rate R (bit/s/Hz) is then

$$P_{\text{out}}(\text{SNR}, R) = \mathbb{P}[\mathcal{I}(\text{SNR}) < R]$$

Numerical Analysis

Table 8: System Parameters

Parameter	Symbol	Default Value
Bandwidth (LTE)	B	20 MHz
Base station antenna gain		30 dB
Fraction of pilot overhead	β	0.5
Distance between adjacent hexagonal cells		$\sqrt{3}$ km
Fractional frequency reuse	Δ	1
Length of cell side	D_{cell}	1 km
Pathloss exponent	η	4
Pathloss offset		-128 dB
Number of forward/reverse link users per cell	K_ℓ	10
BS density	λ_{BS}	0.1 BS/km^2
UE density	λ_{UE}	0.5 UE/km^2
Number of antennas	N_{a}	100
Number of fading coherence tiles	N_{c}	20,000 (Pedestrians)
Number of pilots per cell	N_{p}	$3K_\ell$
Noise figure		3 dB
Forward link transmit power		40 W
SI channel power	μ_{SI}	10 dB
SI power	P_{SI}	40 W
Reverse link transmit power		200 mW
Shadowing	σ_{dB}	8 dB
Thermal noise spectral density		-174 dBm/Hz
Reverse fractional power control	ϑ	0.7
Forward power allocation	ϑ	0.0 (uniform)
Carrier frequency (mmWave)		28 GHz
Bandwidth (mmWave)		850 MHz
Number of clusters	C	6
Number of rays per cluster	R	8
AoA/AoD angular spread		20°
Transceivers gap	d	2λ
Transceivers incline	ω	$\frac{\pi}{6}$
Rician factor	κ	5 dB

- For hexagonal grid, we consider a two-tier network, i.e., 19 cells
- For square grid, we consider 25 cells

Cumulative Distribution Function (Forward Link SQINR)

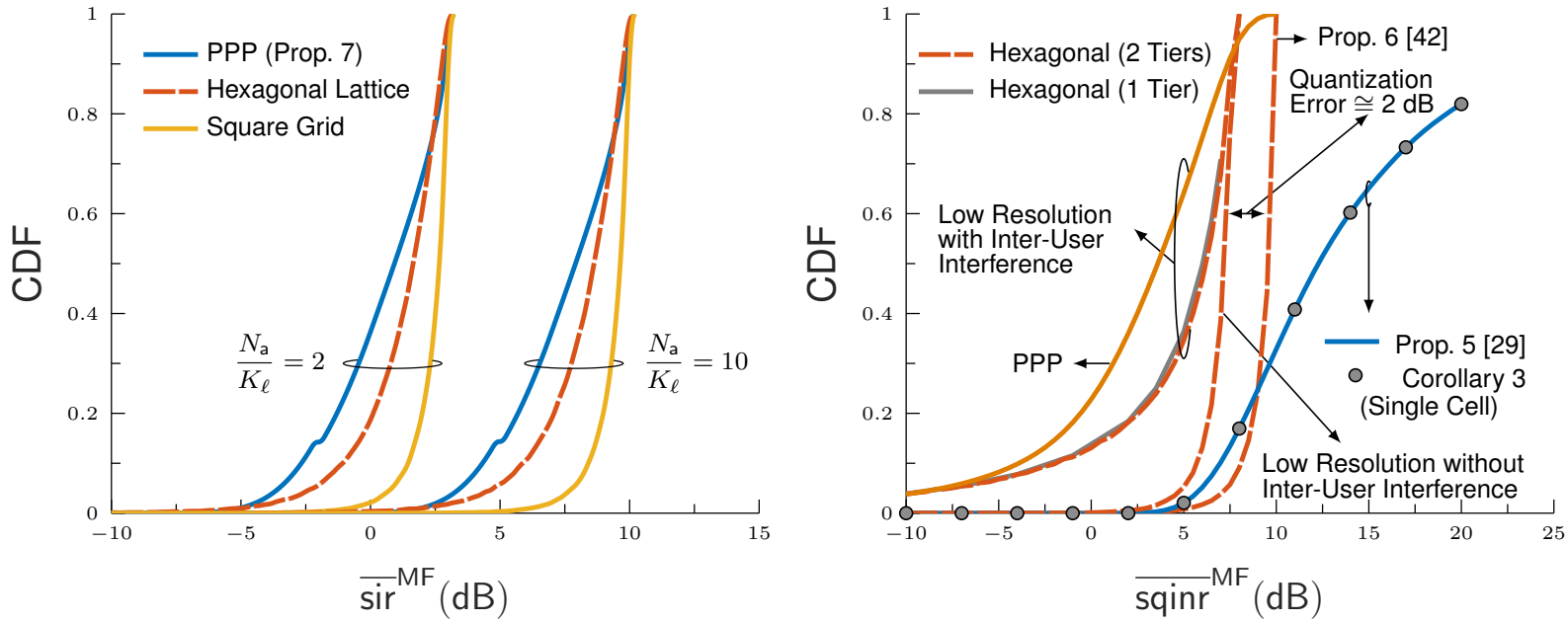

- (Left) Gap between Hexagonal, square and PPP is less than 2 dB
- (Left) If the shadowing and # cells increase, the gap shrinks as the simulation curves converge to their analytical counterparts
- (Right) PPP exceeds Hexagonal, except for a small range of $5 - 8$ dB
- (Right) Inter-user interference degrades the performance
- (Right) 2 dB loss incurred by the quantization noise

Spectral Efficiency and CDF

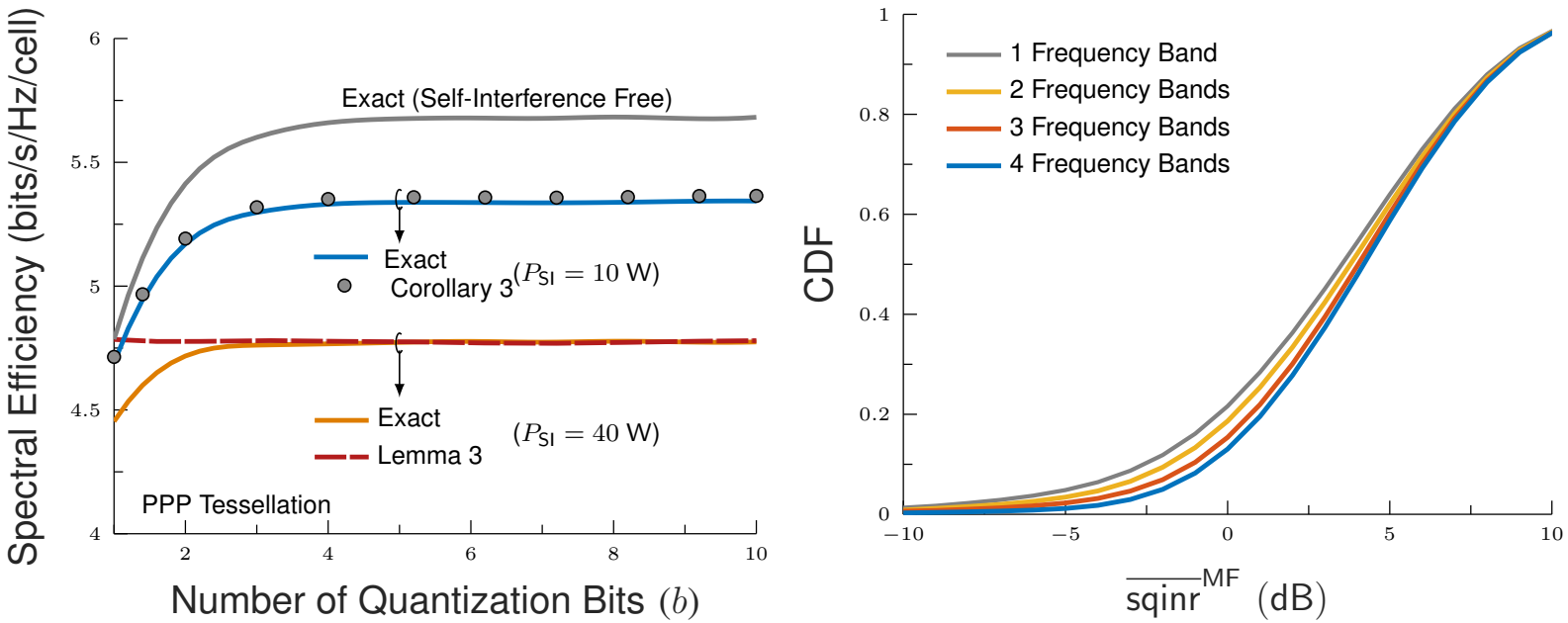

(a) Reverse link. (b) Forward link

- (Left) SI power degrades the performance
- (Left) 4 quantization bits achieves the full-resolution results
- (Right) Increasing # bands improve the CDF as it decreases the interference, however, it degrades the spectral efficiency

Contribution #5: Multiuser Massive MIMO Full Duplex Hybrid Beamforming Cellular Networks

- **Problem**: Design full-duplex systems for cellular networks in practical scenarios
- **Approach**: Quantify effects of self-interference and a wide range of other impairments on communication performance
- **Proposed Solution**: Develop unified framework for analysis of effects of network irregularities on communication performance in sub-6 GHz and mmWave bands
  - Hardware impairments such as quantization noise
  - Pilot contamination
  - Self-, inter-user, and inter-cell interference
  - Reverse and forward links
  - Power scaling laws, asymptotic analysis and special cases
- **Takeaways**:
  - Reverse link: 4 quantization bits achieve full-resolution results
  - Forward link: Power scaling laws show using more antennas can eliminate inter-user, inter-cell & intra-cell interference, pilot contamination, noise.

The University of Texas at Austin
Cockrell School of Engineering